# Highlighting the significant potential of $Nb_2O_5$ and a-C coatings to improve the wear and corrosion resistance of 316L stainless steel

M.O.A. Ferreira[1], K.R. Santos[1], F. E. Mariani[2], R.V. Gelamo[3], N. B. Leite Slade[4], M.M. Morais[5], C.A. Fortulan[5], H.C. Pinto[1], J.A. Moreto[1*]

[1]Materials Engineering Department, São Carlos School of Engineering, University of São Paulo (USP), São Carlos, São Paulo, Brazil.
[2]Department of Production Engineering, São Carlos School of Engineering, University of São Paulo (USP), São Carlos, São Paulo, Brazil.
[3]Institute of Technological and Exact Sciences, Federal University of Triângulo Mineiro (UFTM), Uberaba, Minas Gerais, Brazil.
[4]Institute of Exact Sciences, Naturals and Education, Federal University of Triângulo Mineiro (UFTM), Uberaba, Minas Gerais, Brazil.
[5]Mechanical Engineering Department, São Carlos School of Engineering, University of São Paulo (USP), São Carlos, São Paulo, Brazil.

*Corresponding author: jamoreto@usp.br

This is a post-peer-review, pre-copyedit version of an article published in [Emergent Materials]. The final authenticated version is available online at: https://doi.org/10.1007/s42247-025-01028-5.

## Abstract

Surface functionalisation using nanostructured coatings represents a promising strategy for enhancing the corrosion and wear resistance of commonly used biomedical metallic implants, such as 316L stainless steel. In this study, we investigated the effects of niobium pentoxide ($Nb_2O_5$) and amorphous carbon (a-C) coatings, which were applied to the surfaces of 316L stainless steel via the reactive sputtering technique. A series of pin-on-disk analyses and electrochemical tests were performed under various environmental conditions. The results clearly indicated that both coatings significantly reduced the coefficient of friction compared to the uncoated alloy when tested in air, 0.6 mol $L^{-1}$ NaCl solution, and artificial saliva. Under all tested conditions, the sample coated with a thin film of $Nb_2O_5$ demonstrated the lowest values for wear volume and wear rate. Measurements of open circuit potential, potentiodynamic polarisation, and electrochemical impedance spectroscopy provided compelling evidence of the effectiveness of reactive sputtering in creating coatings that markedly enhance the resistance of 316L stainless steel to uniform corrosion processes when exposed to 0.6 mol $L^{-1}$ NaCl and artificial saliva solutions.

**Keywords:** Surface functionalisation, Reactive sputtering, Nanostructured coatings, Wear behaviour, Corrosion tests.

## Highlights

- Niobium pentoxide and amorphous carbon coatings were fabricated by using DC sputtering;
- The produced coatings offer significantly enhanced wear resistance for 316L stainless steel;
- Nanostructured coatings enhanced 316L stainless steel's resistance to uniform corrosion.

## Graphical Abstract

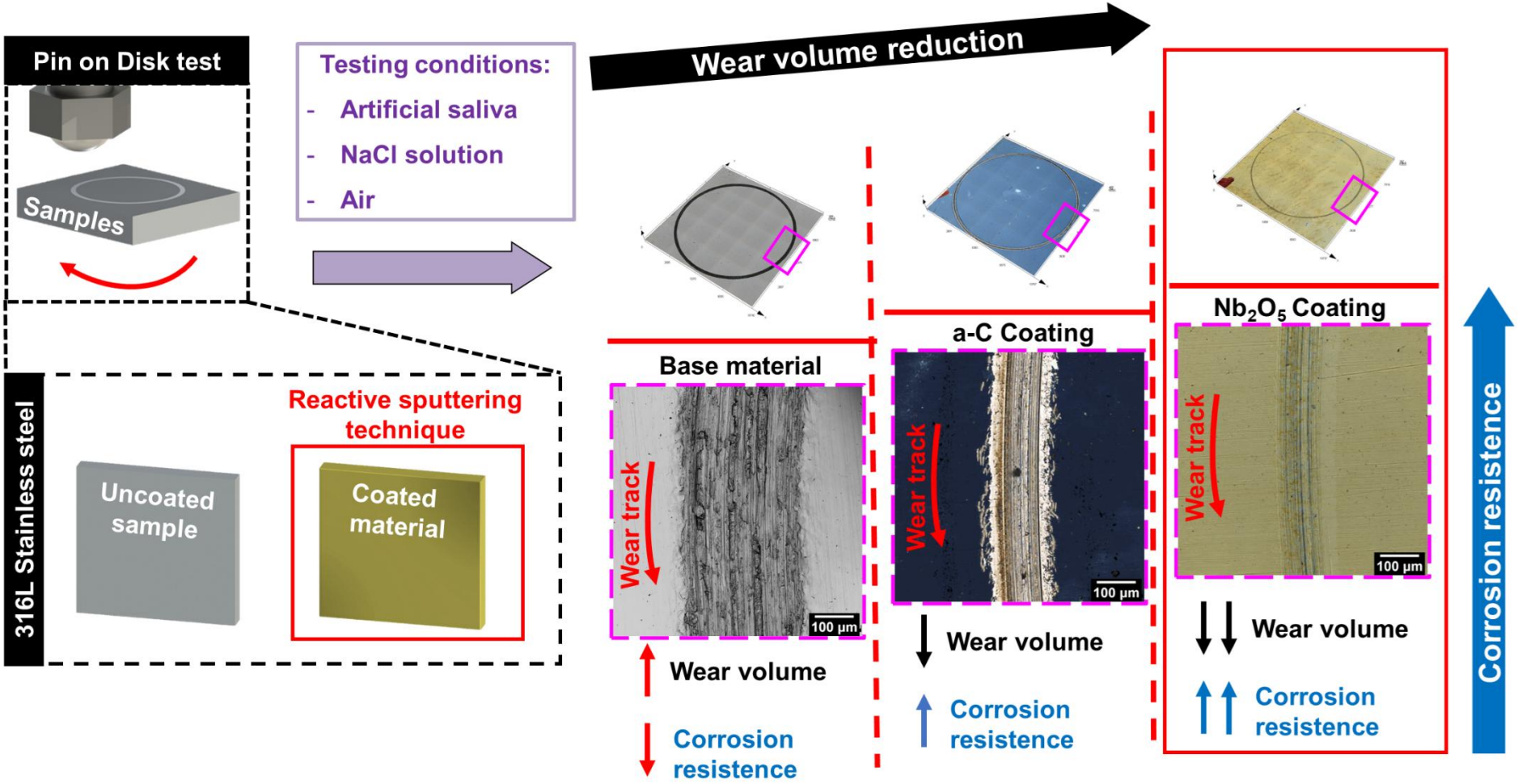

## 1. Introduction

The 316L stainless steel is widely used across various sectors owing to its exceptional properties. Biomedical engineering, petrochemical, and automotive are examples of areas where the remarkable mechanical, anticorrosive, and biological properties of 316L stainless steel are being explored **[1]**. Furthermore, considering the commercially available metallic alloys used for implant applications in the biomedical industry like titanium, magnesium, and cobalt-based materials the 316L stainless steel offers lower cost, simplicity, and a variety of fabrication processes **[2,3]**. Furthermore, there is a growing interest in utilizing these materials for biomedical applications as a replacement for the conventional and widely used Ti-6Al-4V alloy. This interest arises not only from the high cost associated with this alloy but also from the presence of potentially harmful elements in its composition, such as aluminium and vanadium, which may pose risks to human health **[4]**.

The good corrosion resistance of 316L stainless steel is attributed to the nano-scale oxide layer that spontaneously forms on its surface upon exposure to the atmosphere **[5, 6]**. However, 316L stainless steel exhibits inferior corrosion resistance and tribological performance in aggressive environments when compared to conventional Ti-6Al-4V titanium-based alloys **[7, 8]**. In the context of the human body, varying concentrations of aggressive ions and fluctuations in pH contribute to the degradation of the passive oxide layer, thereby promoting various localised corrosion processes, such as pitting **[9-12]**. Furthermore, as is well established in the literature, that the combined effects of wear and corrosion can significantly accelerate the surface degradation of 316L stainless steel, ultimately resulting in a significant reduction in the material's service life **[13, 14]**. Considering the above, it is imperative to enhance the resistance of this alloy against to localised corrosion while also improving its wear properties. Such advancements are crucial for expanding the use of 316L stainless steel as a biomaterial for orthopedic implants shortly **[15-17]**.

In this context, an intriguing approach involves employing surface modification techniques to improve the wear resistance, biofunctional, and corrosion behaviour of 316L stainless steel **[16, 17]**. A variety of techniques, such as electrodeposition **[18-21]**, anodising processes **[22, 23],** green inhibitors implementation **[24, 25],** laser-based treatments **[26, 27]**, plasma enhanced chemical vapor deposition (PECVD) **[28]**, and physical vapor deposition (PVD) **[29, 30, 31]** have been thoroughly investigated in recent years, yielding promising results.

Laybidi and Bahrami **[19]** employed the electrophoretic deposition technique to fabricate bioactive glass coatings containing ZnO on 316L stainless steel substrate for biomedical applications. The authors successfully generated a dense coating layer characterised by homogeneity and uniform elemental distribution, preserving the surface morphology - a determinant factor for the efficacy of implantable devices. Furthermore, the antibacterial activity of the various coatings with differing ZnO concentrations was evaluated against *Escherichia coli* and *Staphylococcus aureus*, demonstrating their potential as protective layers for metallic implantable devices. Despite the promising results reported by the authors, it is important to note that the electrophoretic deposition of aqueous suspensions may present certain challenges related to water electrolysis, which can lead to bubble entrapment within the oxide layer and result in substandard coating quality **[32]**.

Additionally, the sol-gel deposition technique is attractive due to its ability to produce films with high homogeneity, purity, and excellent uniformity in various colloidal mixtures, typically involving complex oxide structures. This facilitates precise control of the chemical composition at the molecular level **[33]**. In this sense, numerous research groups have been exploring the sol-gel technique's potential for forming various compositions of protective films on a range of biomaterial substrates, such as 316L stainless steel **[34, 35, 36]**. The most deposited nanocomposite using this method is hydroxyapatite-based structures, owing to their favourable biocompatibility in bone and cartilage implantable devices. Sirajunisha and collaborators **[35]** have evaluated the impact of a sol-gel deposited Ti-rGO-HAp nanocomposite system on several properties of 316L stainless steel, specifically for biomedical applications. The authors report that this nanocomposite improved the cell viability of the 316L stainless steel and enhanced its effectiveness against various bacterial strains. Despite its benefits, the sol-gel technique often forms greater thickness films with higher pore density **[37]**, which is undesirable for protective coatings, as these pores can facilitate the interaction of the metallic substrate with corrosive ions in the environment.

As with the bifunctional properties of implantable devices, the mechanical surface performance of biomedical materials is a critical determinant of implant success **[38]**. In this context, the application of laser-based treatments to metallic materials in the biomedical field is particularly appealing, as these treatments allow for the precise modification of surface properties, thereby tailoring them for specific applications **[39, 40, 41]**. Filano and colleagues **[39]** examined the use of the laser shock peening technique

to enhance the corrosion resistance and mechanical properties of 316L stainless steel, as well as to evaluate the synergistic effect of the oxide layer in a biological environment. Following the laser shock peening treatment, the 316L stainless steel samples exhibited a 68% reduction in corrosion current rate compared to untreated surfaces in Hank's solution. However, according to the authors, this surface treatment resulted in increased surface roughness relative to the base material, which can pose challenges for implantable devices by impacting cell adhesion and biofilm formation due to alterations in the surface finish of the metallic material.

Numerous studies conducted by this research group have underscored the exceptional properties of $Nb_2O_5$ and a-C coatings deposited via the PVD technique, aimed at enhancing the uniform and localised corrosion processes, wear, fatigue, corrosion-fatigue, and biological properties of 316L stainless steel, aluminium, and titanium alloys **[30,42-48]**. The PVD technique has demonstrated considerable promise in producing compact and homogeneous coatings with strong adhesion to various metal substrates. Additionally, it is regarded as an eco-friendly and cost-effective approach. Among these studies, the work of Nascimento and colleagues **[44]**, which assessed the influence of the $Nb_2O_5$ thin film on the biological response of Ti-6Al-4V alloy, constitutes a notable contribution to the application of such coatings on metallic materials. In reference **[44]**, the authors investigated the effects of $Nb_2O_5$ coating on the Ti-6Al-4V alloy through various methods, including the differentiation of osteoblastic cell line MC3T3-E1, cell proliferation, alkaline phosphatase analysis, biomineralization tests in simulated body fluid, and assessments of antibacterial activity. The results indicated that the $Nb_2O_5$ film enhanced the cellular response of MC3T3 osteoblast cells and demonstrated antibacterial activity, alongside other crucial bioactive properties such as cell viability, adhesion, and growth on the surface of the Ti-6Al-4V alloy. In reference **[30],** the authors evaluated the effect of the $Nb_2O_5$ coating on the biological response of 316L stainless steel concerning gingival cells (HGF-1 cell line), reporting exceptionally positive outcomes, as the $Nb_2O_5$ coating exhibited lower toxicity and induced reduced levels of cell inflammation compared to the uncoated material.

Moreover, various research groups in the literature have corroborated the advantageous biological properties of different coatings deposited by the PVD technique on 316L stainless steel **[50-53]**. Fróis and colleagues investigated the influence of nitrogen-doped particles on the a-C:H thin film deposited on the 316L stainless steel substrate by using the sputtering technique, specifically in terms of its biological response

**[50]**. The results of the cell viability assay demonstrated that all coated samples were biocompatible, as their medians exceeded the 70% level regarding the control. The excellent biocompatibility of 316L stainless steel was further enhanced following surface modification through the deposition of carbon materials, with or without the addition of nitrogen. Additionally, studies assessing the release of metal ions in a Fusutama-Meyer solution, a simulated acidic saliva modified according to the ISO 10271 protocol, revealed that the coated samples exhibited lower degradation when compared to the uncoated material. Senocak et al **[53]** examined the impact of PVD-deposited niobium-oxynitride coating on the antibacterial properties and in vitro cytotoxicity of 316L stainless steel. By modifying the PVD parameters, the authors evaluated the effects of different $NbO_x$-$N_y$ structural types on the biocompatibility of 316L stainless steel. All coated samples showed an approximate 25% increase in biological activity compared to the base material, indicating enhanced cell adhesion and proliferation. This variation in the crystallinity of $NbO_x$-$N_y$ structures influenced bacterial adhesion; specifically, a more crystalline structure facilitated lower bacterial diffusion compared to the amorphous and crystalline-amorphous variants. As noted by the authors and supported by XRD analysis, this difference in crystallinity is attributed to a higher content of $Nb_2O_5$ within the coating's crystal structure. These findings underscore the viability and promise of PVD-deposited niobium and amorphous carbon-based coatings in inducing improved biological responses in implantable devices.

Ferreira et al **[49]**, evaluated the influence of nanostructured $Nb_2O_5$ and a-C coatings, deposited by using the reactive sputtering technique, on the corrosion properties of 316L stainless steel in 0.6 mol $L^{-1}$ NaCl solution. The results showed that both coatings significantly improved the corrosion performance of the 316 L SS by providing a safety margin between the corrosion potential ($E_{corr}$) and the pitting potential ($E_{pitting}$). Additionally, following 48 h of immersion in 0.6 mol $L^{-1}$ NaCl solution, the 316L stainless steel samples with both coatings exhibited significantly higher impedance moduli compared to the uncoated sample, which was observed after only 3 h of immersion. However, there exists a significant paucity of studies within the international literature that investigates the effects of promising $Nb_2O_5$ and a-C coatings on the tribological behaviour of 316L stainless steel. This gap in research is particularly concerning given the potential of these coatings to enhance the corrosion and wear resistance of 316L stainless steel, thereby improving the longevity and performance of biomedical implants. A thorough examination of their impact on tribological properties is

essential for understanding their applicability in practical scenarios and for enabling advancements in the field of biomaterials.

In this study, we present innovative applied research that aims to investigate the effects of $Nb_2O_5$, and a-C coatings deposited via the reactive sputtering technique on the surfaces of 316L stainless steel, with the objective of enhancing wear and corrosion properties. To achieve this goal, a series of pin-on-disk analyses were conducted under various environmental conditions, including air, following exposure to a 0.6 mol $L^{-1}$ NaCl solution, and artificial saliva. Furthermore, an extensive morphological analysis of the wear track was conducted by using a confocal laser scanning microscope (CLSM) and a scanning electron microscopy/energy-dispersive X-ray spectroscopy (SEM/EDX). The electrochemical behaviour of 316L stainless steel, both with and without $Nb_2O_5$ and a-C coatings, was assessed using open circuit potential (OCP), potentiodynamic polarisation curves (PPc), and electrochemical impedance spectroscopy (EIS) in 0.6 mol $L^{-1}$ NaCl and artificial saliva solutions.

To the best of our knowledge, this study represents the first investigation in the literature regarding the tribological properties of 316L stainless steel containing $Nb_2O_5$ and a-C nanostructured coatings produced through the reactive sputtering technique. Furthermore, it provides a comprehensive comparison of the electrochemical behaviour of these coatings in both sodium chloride and artificial saliva solutions, offering valuable insights into their potential applications in biomedical contexts.

## 2. Experimental

### *2.1 Material*

In the current study, the 316L stainless steel were used in their as-received condition and with nominal chemical compositions of Cr 17.4%, Ni 9.8%, Mo 2.5%, Mn 1.6%, Si 0.5%, and Fe balance (% in weight), already determined in a previously published work **[49]**. Prior to the reactive sputtering deposition process, the 316L stainless steel samples were cut into standard sizes of 2 cm x 2 cm via electrical erosion process. The samples were then ground using silicon carbide (SiC) abrasive paper with a grit range of 800, 1200, 2400 and 4000#. This was followed by polishing with diamond pastes of 3, 2, and 1 μm. Finally, the samples were washed in distilled water and isopropyl alcohol for 15 min each. Subsequently, all samples were placed in appropriate sample holders for corrosion and wear testing.

### *2.2 Deposition process*

For the deposition, a DC-magnetron sputtering chamber was employed, equipped with 2-inch diameter targets of Niobium (99.99%) and *Highly Oriented Pyrolytic Carbon* (HOPG) , operating in the same temperature of 300 $^{o}$C. For the $Nb_2O_5$ thin film, the chamber atmosphere consisted of a mixture of argon (99.99%) and oxygen (99.99%) at 5.0 and 0.5 mTorr, respectively, with an applied voltage of 440 V and current of 140 mA. For the a-C coating, the electric current and applied potential were 170 mA and 600 V, respectively. Further details regarding the deposition process and the characterisation of both coatings can be found in the references **[30, 42, 49]**. As reported by reference **[49]**, the analysis of the functionalised niobium oxide-based coating ($Nb_xO_y$) reveals that it is predominantly composed of $Nb_2O_5$, with minor amounts of NbO and $NbO_2$. Considering a-C thin films, Raman spectroscopy (RS) and X-ray photoelectron spectroscopy (XPS) reveal the presence of the characteristic D and G bands, alongside significant contributions from C-C and C-H bonds, respectively. Furthermore, the coating thicknesses were determined using profilometry and atomic force microscopy techniques (AFM). Based on this information, from this point forward, the samples featuring niobium oxide thin films will be referred to as $Nb_2O_5$.

### *2.3 Pin-on-disk sliding wear tests*

In the present study, wear tests were performed on 316L stainless steel, as well as on 316L stainless steel containing $Nb_2O_5$ and a-C coatings. For this purpose, the specimens were positioned in the centre of a pin-on-disk tribometer and subjected to wear resistance testing under various conditions, in accordance with ASTM-G99-23 standards **[54]**. **Figure 1** depicts a schematic drawing of the tribometer used for the pin-on-disk analysis. Microadhesive wear measurements were performed in triplicate maintaining a constant load (5 N), a track diameter between 9 and 10 mm, and a sliding velocity of 0.01 m $s^{-1}$, using alumina spheres with a diameter Ø = 4.78 mm. In addition, wear tests of varying durations were conducted to evaluate the effectiveness of both coatings in improving the wear resistance of the 316L stainless steel.

All samples underwent evaluation at three environmental conditions: in air, after immersion in 0.6 mol $L^{-1}$ NaCl solution for 2 h, and after immersion for 2 h in artificial saliva solution. The latter consist of various chloride compounds, sodium saccharin, 2-bromo-2-nitropropane-1,3-diol, xylitol, potassium dihydrogen phosphate, flavor, citric acid, PEG40, and purified water. Morphological analysis and wear track examination of

all samples were performed using an Olympus confocal laser scanning microscope (CLSM), model OLS4100, as well as a Tescan scanning electron microscope (SEM) model MIRA2, coupled with an Oxford X-ray energy-dispersive spectroscopy (EDX) system. Furthermore, the wear volume was calculated in accordance with ASTM G99-23 guidelines to evaluate the coatings' effectiveness in protecting the 316L stainless steel against wear **[54]**. All wear analyses were performed at the Laboratory of Tribology and Composites at the São Carlos Engineering School (EESC) at University of the São Paulo (USP), São Paulo State, Brazil.

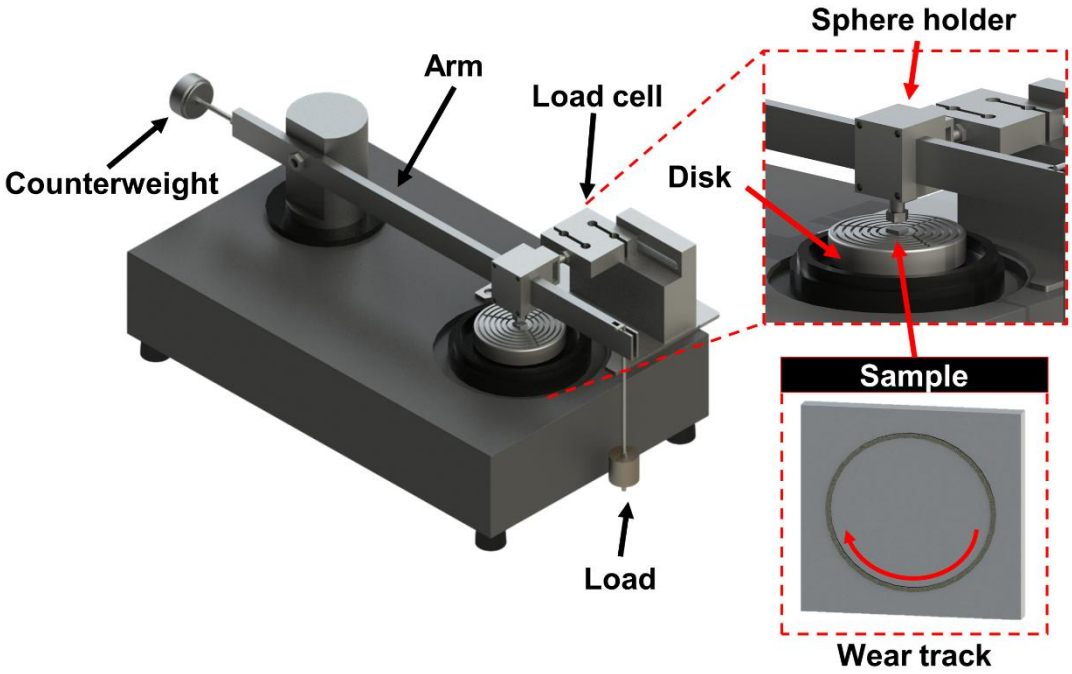


**Figure 1.** Schematic illustration of the pin-on-disk apparatus used in this present study, highlighting its major components including the load application system, counterweight, arm, load cell, rotating disk, sphere holder, and the wear track formed. **Figure 1** was adapted from reference **[31]**.

### *2.4 Corrosion tests*

To fully evaluate the $Nb_2O_5$ and a-C coatings performance on protecting the 316L stainless steel substrate under different environments, OCP, PPc, and EIS techniques were used in the present work. To this end, a conventional electrochemical cell was employed, comprising three electrodes: the working electrode consisting of both uncoated and coated 316L stainless steel specimens with an exposure area of approximately 0.20 $cm^2$, a platinum counter electrode (CE), and a saturated calomel reference electrode (SCE) ($Hg/Hg_2Cl_2$, $KCl_{sat}$), using a μStat-i-400s (Bi) potentiostat/galvanostat. The corrosion

tests were performed by using 0.6 mol $L^{-1}$ NaCl and artificial saliva solutions. Moreover, at least three samples for each condition were tested to ensure the reliability and reproducibility of the results obtained in this study. The open circuit potential ($E_{ocp}$) was monitored during 2 h until for each studied system. The PPc were obtained in the range of -0.4 to 1.2 V/SCE with a potential sweep rate of 0.1 $mVs^{-1}$. Following, the EIS spectra were acquired for a frequence range of 100 kHz to 10 mHz using an applied a.c. signal of 10 mV (rms) at room temperature. Following the PPc tests, a series of optical microscope (OM) analyses were performed to gather information on the surface characteristics of both uncoated and coated 316L stainless steel samples. All electrochemical tests and morphological analyses were conducted in the Materials Engineering Department (SMM) at the São Carlos School of Engineering (EESC), University of São Paulo (USP), São Paulo state, Brazil.

## 3. Results & Discussions

**Figure 2** displays profilometry measurements and respective AFM images of the 316L stainless steel surface with both $Nb_2O_5$ and a-C coatings. Comparing the results of the profilometry analysis is possible to verify that the $Nb_2O_5$ thin film possesses a higher thickness in comparison to the a-C coating (240.0 ± 10 nm *versus* 38.2 ± 14 nm). As already verified in references **[30,42-43,49]**, a thicker and defect-free coating such as the $Nb_2O_5$ can positively influence the uniform and localised corrosion processes as well as mechanical performance of metallic substrate in comparison to a more lass thicker coating.

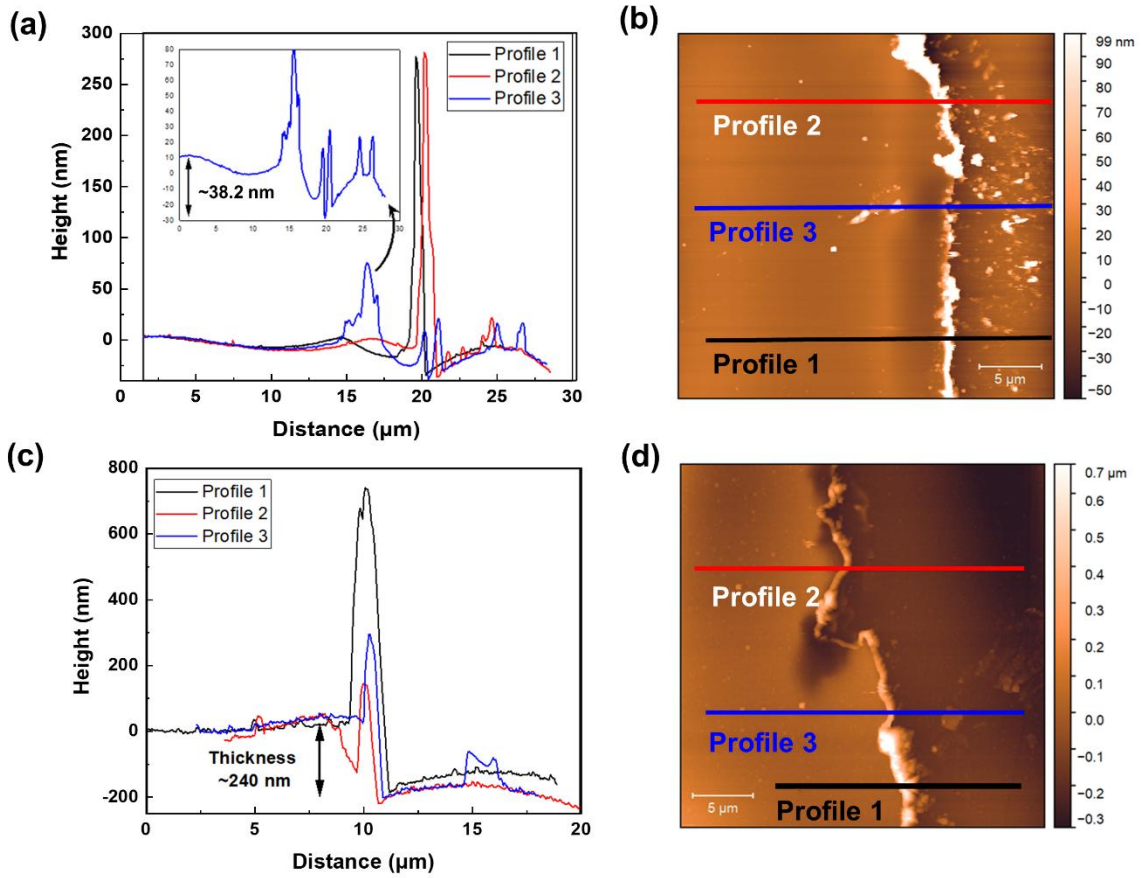


**Figure 2.** Profilometry measurements and corresponding AFM images for **(a, b)** a-C and **(c, d)** $Nb_2O_5$ coatings deposited on the surface of 316L stainless steel by using reactive sputtering technique.

**Figures 3 (a-d)** present the results of the coefficient of friction obtained by the pin-on-disk tests, regarding three conditions: in air, after immersion in 0.6 mol $L^{-1}$ NaCl, and after immersion in AS. First, considering the 316L stainless steel, is verified a stabilization period on the coefficient of friction values for all the tested conditions until 100 s, approximately. Likewise, the increase in coefficient of friction values can be attributed to the interaction between the sphere and the rough surface of the 316L stainless steel, which resulted from the polishing procedure utilised during sample preparation **[55]**. However, as the sphere interacts with the metallic surface and passes this superficial layer, after around 100 s, the coefficient of friction corresponds to the actual interaction of the $Al_2O_3$ sphere and the 316L stainless steel matrix. To elucidate the impact of the coatings on the wear performance of 316L stainless steel, **Table 1** summarises the average values of the coefficient of friction for each sample under the specific conditions analysed. Additionally, for both coatings, the coefficient of friction values are reported for the initial phase of the experiment as well as those recorded after film rupture. It is important to

note that all experimental data included in this work are accompanied by comprehensive statistical analyses. This not only validates the results reported here but also confirms that both coatings significantly enhance the wear performance of 316L stainless steel. In comparison, the uncoated material exhibited coefficient of friction values across all tested conditions ranging from 0.40 to 0.45, with no statistically significant variation, as indicated in **Table 1**.

Regarding the 316L stainless steel containing $Nb_2O_5$ coating, several noteworthy time frames must be addressed for all tested environments. Firstly, for the analysis in air, the average coefficient of friction value is significantly lower during the first 700 s when compared to the uncoated material, as shown in **Figure 3 (a)**. As reported in the literature **[42, 46, 56]**, this reduction is primarily attributed to the hardening of the coating and its ability to alter the surface roughness and reduce its interaction with the $Al_2O_3$ sphere. Moreover, this modification was also observed in the variance of the coefficient of friction values in all conditions for the $Nb_2O_5$ coating, where the variance reduced from 0.05 to 0.02 in comparison to the uncoated samples, see **Table 1**. After 700 s and up to 850 s, a drastic change in the coefficient of friction values is observed, with a similar profile to the stabilization zone for the uncoated sample. This implies that the sphere has reached the interface between the coating and the 316L stainless steel polished surface. Additionally, until the end of the experiment, the coefficient of friction values was around 0.40, very similar to the uncoated 316L stainless steel, see **Table 1**.

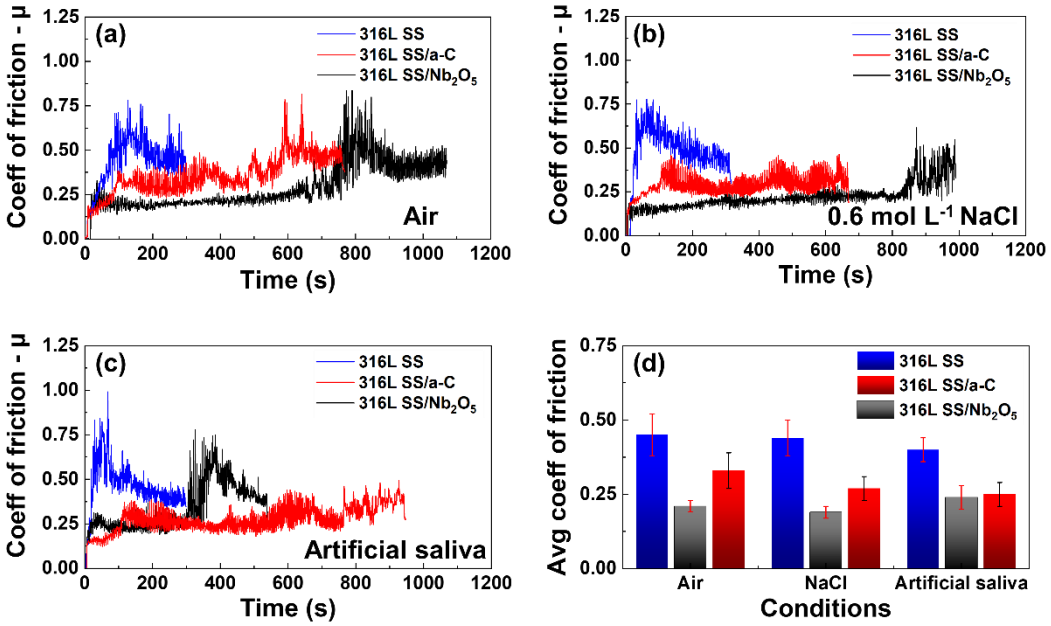


**Figure 3.** Coefficient of friction of 316L stainless steel without and with the $Nb_2O_5$ and a-C coatings for different conditions: **(a)** air, **(b)** after 2 h of immersion on 0.6 mol $L^{-1}$ of

NaCl, **(c)** after 2 h of immersion on AS and **(d)** comparison average coefficient of friction for all the tested materials.

Considering the 316L stainless steel /$Nb_2O_5$ sample after exposure to 0.6 mol $L^{-1}$ NaCl solution, the coefficient of friction values remained lower than the uncoated 316L stainless steel and very similar to those observed in air, with the film breaking occurring around 800 s, as illustrated in **Figure 3 (b)**. The same phenomenon can be observed, in which the $Nb_2O_5$ film promotes a reduction in the interaction between the sphere and the metallic substrate, in addition to presenting a higher hardness than the 316L stainless steel **[17,57]**. However, upon examining the curve after immersion in artificial saliva, the transition from the coating to the metallic surface occurs earlier, around 350 s. This indicates that artificial saliva represented the most detrimental environment for the $Nb_2O_5$ coating. Nonetheless, it is important to note that wear predominantly occurred on the coating rather than on the 316L stainless steel substrate. This finding underscores the considerable potential of the $Nb_2O_5$-based coating to extend the wear lifespan of biomedical implants by reducing the average coefficient of friction values.

Regarding the 316L stainless steel /a-C sample, an intermediate behaviour compared to the other two samples can be observed. The average coefficient of friction values of this sample fall between those of the bare material and the 316L stainless steel /$Nb_2O_5$. In experiments conducted in air, the a-C film exhibited significant variation in the coefficient of friction values throughout the experiment, ranging from 0.25 to 0.35, as shown in **Figure 3 (a)**. This can be attributed to a similar effect of modifying the hardness of the coating and the surface roughness of the 316L stainless steel, albeit on a smaller scale compared to the $Nb_2O_5$ coating. Additionally, a discontinuity in the trend of coefficient of friction values is observed around 650 s, followed by stabilization at 0.48, indicating film breaking, like the 316L stainless steel sample. For the measurements after immersion in 0.6 mol $L^{-1}$ NaCl solution, the same variation pattern observed in the air is noted, with film breaking occurring around 600 s (see **Figure 3 (b)**). The results of the analysis after immersion in artificial saliva for 2 h demonstrated that the wear behaviour of the a-C coating remains the same with a film breaking near to 600 s, (**Figure 3 (c)**) Finally, for all analysed conditions, the positive effect of both coatings in protecting the 316L stainless steel substrate is clear.

**Table 1.** Average values of the coefficient of friction for all the analysed samples and conditions.

| Conditions | 316L stainless steel | 316L stainless steel /$Nb_2O_5$ | 316L stainless steel /a-C |
|---|---|---|---|
| **Air** | 0.45 ± 0.07 | 0.21 ± 0.02<br>0.40* ± 0.09 | 0.33 ± 0.06<br>0.48* ± 0.06 |
| **0.6 mol $L^{-1}$ NaCl** | 0.44 ± 0.06 | 0.19 ± 0.02<br>0.41* ± 0.11 | 0.27 ± 0.04<br>0.48* ± 0.05 |
| **Artificial saliva** | 0.40 ± 0.04 | 0.24 ± 0.04<br>0.41* ± 0.04 | 0.25 ± 0.04<br>0.38* ± 0.04 |

*Values after film breaking

**Figure 4** depicts a compilation of CLSM images for all tested conditions and samples for the first 300 s of the experiment. Upon comparing the wear track profiles in the air (see **Figures 4 (a, d, g)**), that the implementation of both coatings promoted a reduction of more than 50% in the wear track width from 240 μm of the uncoated material to 110 μm and 130 μm for the $Nb_2O_5$ and a-C coating, respectively, corroborating the coefficient of friction data. As the coefficient of friction decreases, the interaction between the $Al_2O_3$ sphere and the sample surface decreases, leading to a reduction in volume removal. The same pattern of reduction in wear track profile is observed for the other two conditions: after immersion in 0.6 mol $L^{-1}$ NaCl solution and artificial saliva. This indicates that, regardless of the environmental condition to which the sample is subjected, the coating acted as a protective barrier that improved the wear properties of the 316L stainless steel. Moreover, by analysing CLSM images, the wear pattern of all the samples is predominantly abrasion of two bodies and, as reported in the literature, is the expected pattern for the 316L stainless steel **[58]**. Considering the uncoated samples after immersion in 0.6 mol $L^{-1}$ NaCl solution and artificial saliva, see **Figures 4 (b)** and **4 (c)**, is possible to identify the presence of several pits on the surface in addition to numerous zones of high interaction of the $Al_2O_3$ sphere and the metallic matrix.

Regarding the 316L stainless steel/a-C coating, a complete removal of the film is observed already after 300 s, as indicated by the colour contrast between the outer surface and the wear track, which matched the coloration of the uncoated material, see **Figure 4 (d-f)**. Additionally, various delaminations and film cracking are evident along the wear track vicinity. This type of film deterioration is likely related to the lower adhesion of the a-C coating to the 316L stainless steel surface **[59-61]**. In contrast, for the 316L stainless steel/$Nb_2O_5$ coating, only small defects or delaminated regions can be identified on the wear track, represented by dark spots. This suggests that the $Nb_2O_5$ coating maintains its integrity even after immersion in different aggressive environments and wear for the first 300 s of the pin-on-disk analysis. However, it is worth noting that the 316L stainless steel/$Nb_2O_5$ sample displayed slightly larger defects after immersion in artificial saliva when compared to the sample immersed in 0.6 mol $L^{-1}$ NaCl solution.

**Figure 5** presents a series of SEM/EDX analyses for the nanostructured $Nb_2O_5$ coating under all tested environmental conditions. **Figures 5 (a-d)** pertain to the 316L stainless steel/$Nb_2O_5$ sample after the pin-on-disk analysis in air, where the high presence of Nb indicates that the film remains intact, and the sphere does not encounter the 316L stainless steel surface. In **Figures 5 (e-l)**, which are related to the 316L stainless steel

/$Nb_2O_5$ after 2 h immersion each in both NaCl and artificial saliva solutions, most of the coating remains undamaged except for some small portions where delamination has occurred. This suggests that the $Al_2O_3$ sphere did not reach the metallic substrate, implying degradation only of the coating and not of the substrate. However, this delamination cannot be attributed solely to the substrate adhesion capacity of the $Nb_2O_5$ film, as it was not observed in the air analyses. Instead, it is likely due to corrosion mechanisms associated with the coated 316L stainless steel in an aggressive medium. In this context, Ferreira and colleagues **[49]** investigated the corrosion performance of $Nb_2O_5$ as a protective coating for 316L stainless steel and proposed a corrosion mechanism based on exposure to 0.6 mol $L^{-1}$ NaCl solution. The aggressive ions present in the environment penetrate through micro-defects in the $Nb_2O_5$ coating, initiating a localised corrosion process at the interface between the film and the surface of the 316L stainless steel. As a result, the adhesion of the film in the vicinity of the corroded area is compromised, leading to delamination. Consequently, when the $Al_2O_3$ sphere meets these vulnerable regions, the film is removed.

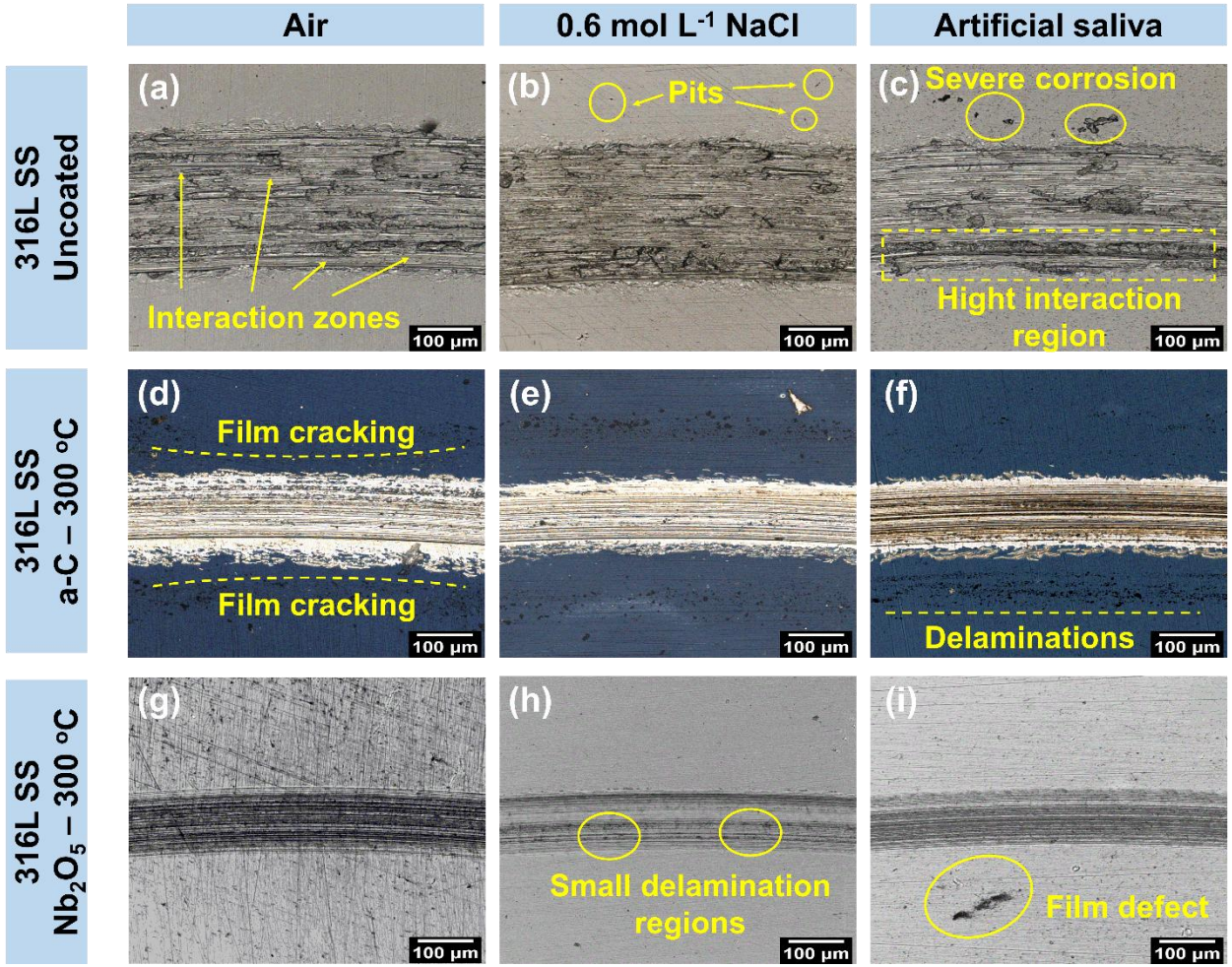


**Figure 4.** CLSM images of **(a-c)** 316L stainless steel, **(d-f)** 316L stainless steel/a-C and **(g-i)** 316L stainless steel/$Nb_2O_5$ considering the different environment conditions.

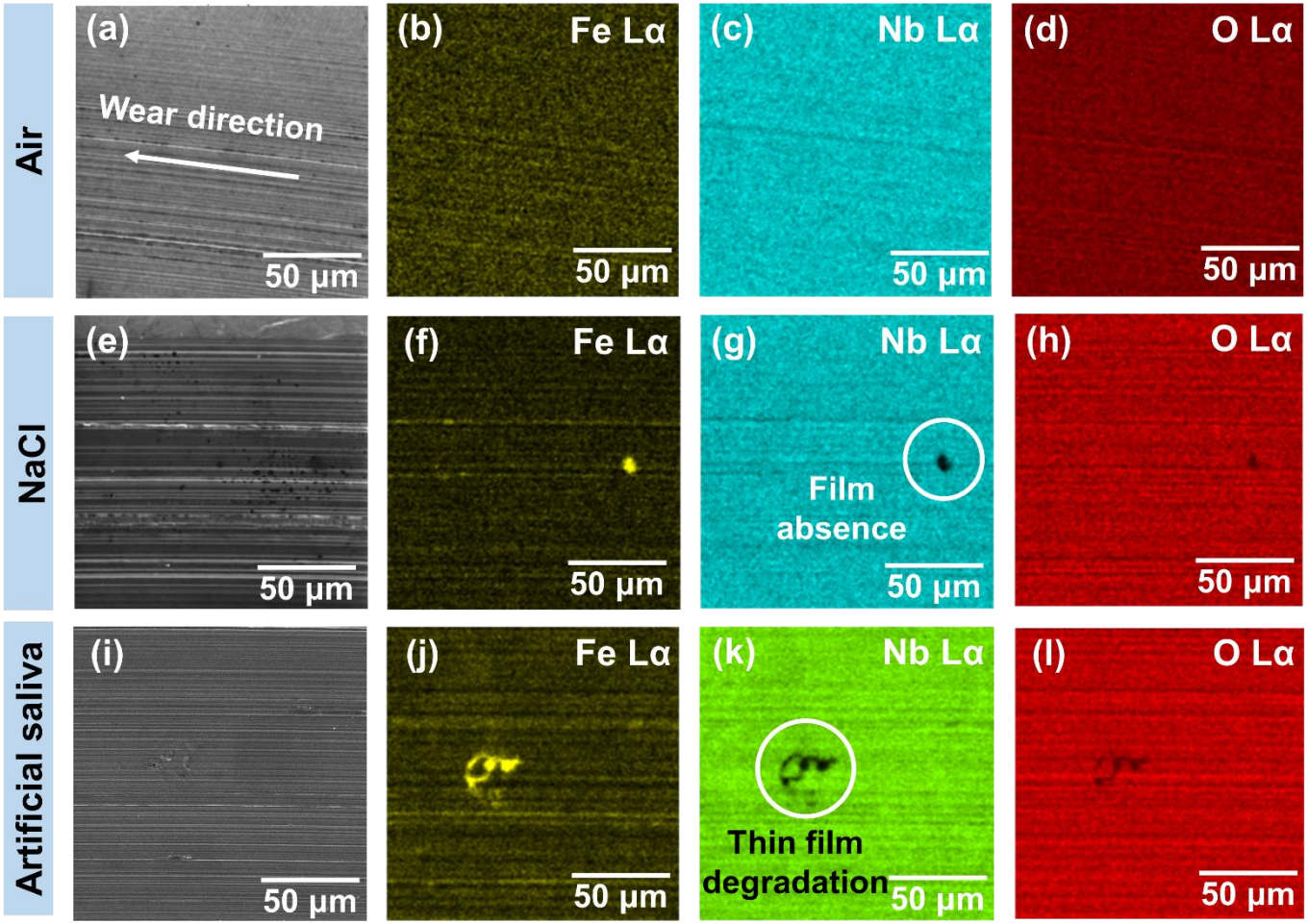


**Figure 5**. SEM images and corresponding EDX maps for the 316L stainless steel/$Nb_2O_5$ under **(a-d)** air, **(e-h)** after 2 h immersion in NaCl solution and **(i-l)** after 2 h immersion on AS.

In addition to the micrograph images displayed in **Figure 4**, a series of measurements of the wear area were obtained by using the Olympus FV10-ASW software, in accordance with the ASTM G99-23. The results presented in **Table 2** are related to the samples in the first 300 s of the pin-on-disk analysis. It is important to mention that, as well as for the coefficient of friction values in **Table 1**, a series of statistical analyses were performed to ensure the validity of the obtained results. Considering the uncoated 316L stainless steel for all the analysed conditions, no significant changes in the wear volume were observed. This indicates that the environment, for small periods of time, does not affect significantly the wear mechanism of these materials. Here, is possible to identify the evident improvement in the wear properties of the 316L stainless steel promoted by the surface functionalisation. The a-C coating exposed to the air and after immersion in NaCl solution promoted a reduction of almost 50% and 65% on the wear rate compared to the bare material, and almost 80% for the artificial saliva condition. Moreover, an even more remarkable reduction is observed for the 316L stainless steel/$Nb_2O_5$ sample in all conditions, where the average wear rate is around 0.2 x $10^{-5}$ $mm^3$ $s^{-1}$, approximately 10% of the wear rate of the uncoated material (20.0 x $10^{-5}$ $mm^3$ $s^{-1}$ in the average). **Figure 6** provides a summary of the data presented in **Table 2** in terms of wear area, facilitating a clearer visualisation of the impact of both coatings on the wear performance of 316L stainless steel under various environmental conditions.

**Table 2.** Average values of wear area, volume, track and wear rate for all the analysed samples considering the different environmental conditions studied.

| Conditions | Samples | Wear area ($\mu m^2$) | Wear track diameter (mm) | Wear volume (x $10^{-3}$ $mm^3$) | Wear rate (x $10^{-5}$ $mm^3$ $s^{-1}$) |
|---|---|---|---|---|---|
| **Air** | 316L stainless steel | 208.5 ± 32.2 | 10.0 | 6.55 ± 1.01 | 2.18 ± 0.34 |
| | 316L stainless steel/a-C | 106.8 ± 31.4 | 10.0 | 3.36 ± 0.98 | 1.12 ± 0.33 |
| | 316L stainless steel/$Nb_2O_5$ | 23.1 ± 1.7 | 9.3 | 0.68 ± 0.05 | 0.22 ± 0.02 |
| **0.6 mol $L^{-1}$ NaCl** | 316L stainless steel | 206.6 ± 39.8 | 9.0 | 5.84 ± 1.13 | 1.95 ± 0.38 |
| | 316L stainless steel/a-C | 77.0 ± 13.8 | 10.0 | 2.42 ± 0.43 | 0.81 ± 0.15 |
| | 316L stainless steel/$Nb_2O_5$ | 21.1 ± 7.3 | 9.6 | 0.63 ± 0.22 | 0.21 ± 0.07 |
| **Artificial saliva** | 316L stainless steel | 204.4 ± 34.1 | 9.4 | 6.04 ± 1.01 | 2.01 ± 0.34 |
| | 316L stainless steel/a-C | 37.0 ± 16.1 | 10.0 | 1.16 ± 0.51 | 0.39 ± 0.17 |
| | 316L stainless steel/$Nb_2O_5$ | 18.3 ± 8.7 | 10.0 | 0.57 ± 0.27 | 0.19 ± 0.09 |

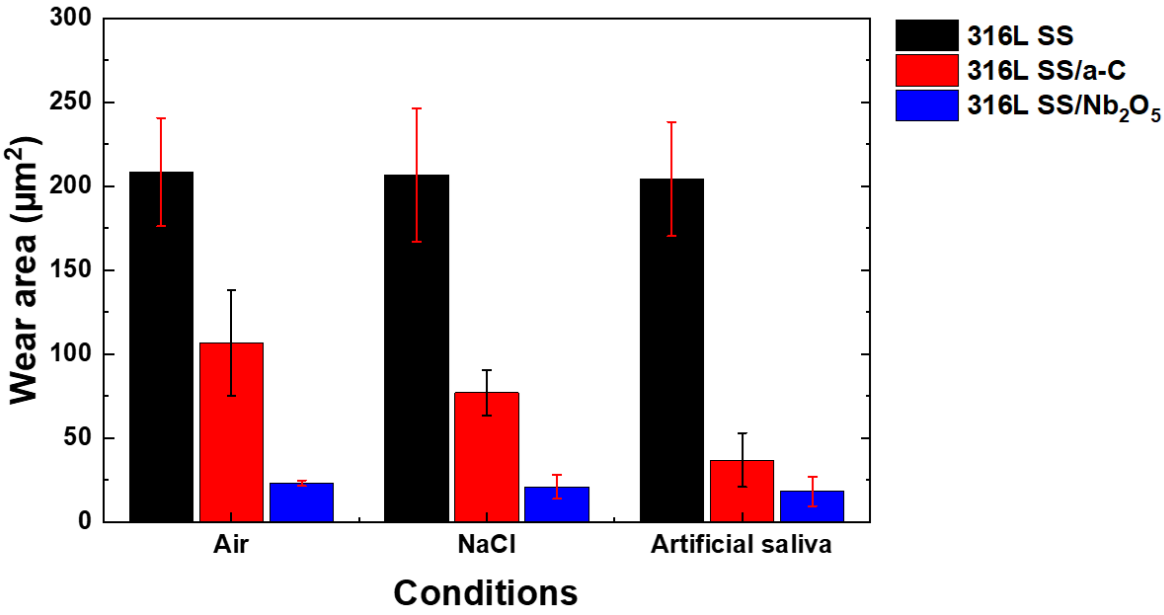


**Figure 6.** Summary graph illustrating the wear area for all tested samples under various environmental conditions.

**Figure 7** provides a summary of the wear mechanisms investigated in this work through a schematic representation. **Figures 7 (a-c)** illustrate the wear profile of uncoated 316L stainless steel, which exhibited the highest wear track under all tested conditions, as confirmed by the CF values and CLSM analysis. **Figures 7 (d-f)** pertain to the 316L stainless steel/a-C, where the wear track width is intermediate, demonstrating a positive performance in protecting the metallic substrate. However, this coating exhibited low adhesion to the 316L stainless steel surface, being completely removed already for 300 s and showing several delaminations, film cracking, and pitting around the wear track. **Figures 7 (g-i)** depict the wear behaviour of the 316L stainless steel/$Nb_2O_5$, with the smallest wear track width and maximum protection of the metallic surface, despite some minor delaminations due to the previously discussed corrosion mechanisms. Finally, all the results presented here along with the wear track morphology analysis demonstrated that the coatings deposited by using reactive sputtering technique were able to improve the wear resistance of the 316L stainless steel. Additionally, the wear performance of the 316L stainless steel/$Nb_2O_5$ is superior when compared to the 316L stainless steel/a-C, as it lasts longer in air and after immersion in 0.6 mol $L^{-1}$ NaCl solution. However, considering the artificial saliva solution, further complementary analysis is necessary to comprehend the phenomena associated with $Nb_2O_5$ film degradation.

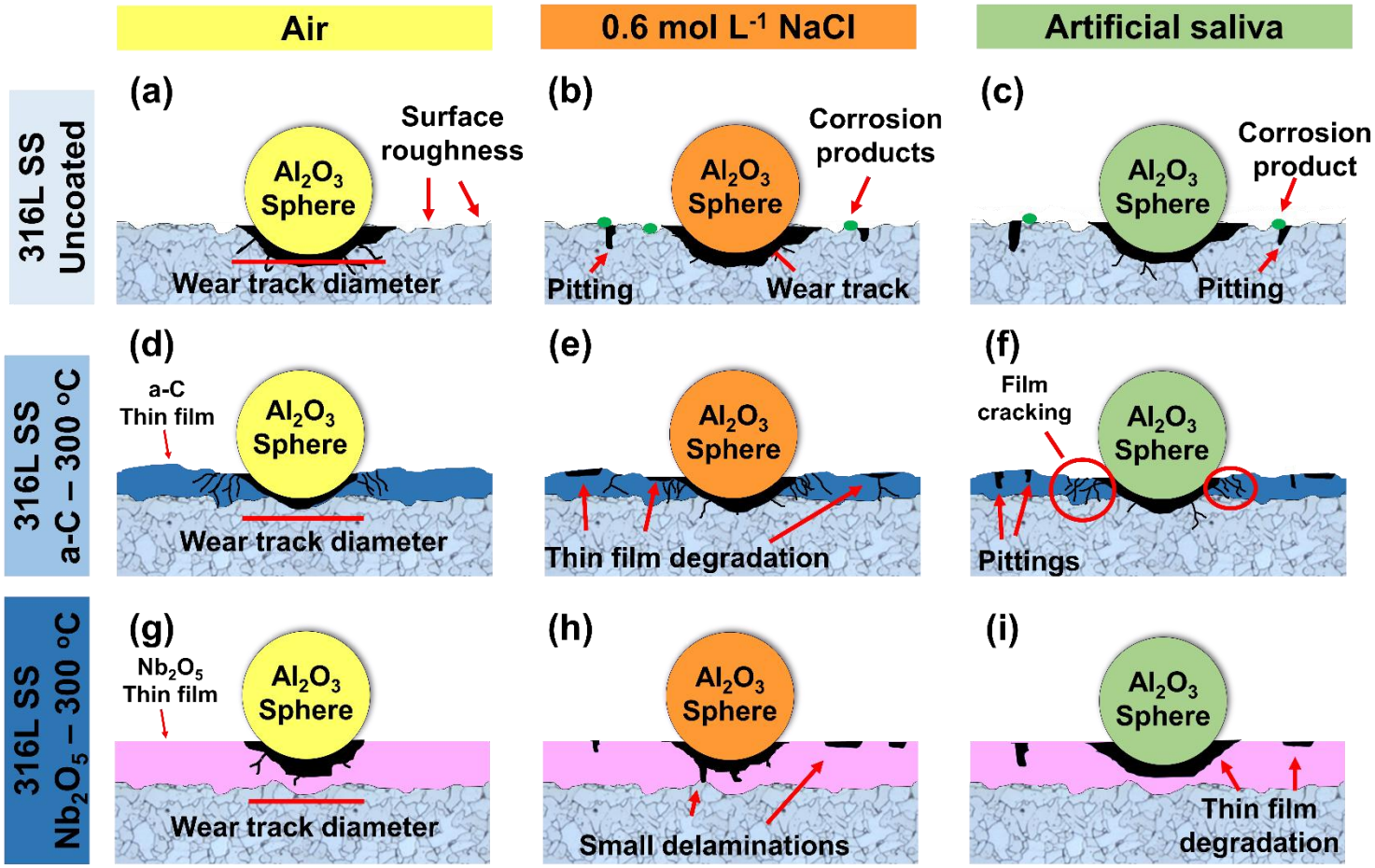


**Figure 7.** Schematical representation of the wear mechanics for the **(a-c)** 316L stainless steel, **(d-f)** 316L stainless steel/a-C and **(g-i)** 316L stainless steel/$Nb_2O_5$ considering the different tested environment conditions

**Figure 8** displays the profilometry analysis of the wear track for all the tested samples surface after the first 300 s of analysis on the pin-on-disk apparatus considering the different environmental conditions. These findings allow a more complete evaluation on the wear track profile, confirming the results previously presented where both coatings promoted an improvement on the wear performance of the 316L stainless steel even in an aggressive environment. In addition, by comparing the performance of both coatings on protecting the substrate is evident that the $Nb_2O_5$ film were more efficient on reducing the wear track diameter and track depth in comparison to the a-C coating. Is worth mention, that even with a lower wear track depth for the sample after immersion in artificial saliva, the uncoated 316L stainless steel sample displayed a higher track diameter in comparison to the coated samples, **Figures 8 (c)**, **(i)** and **(f)**, and consequently a higher wear volume.

**Figure 9** presents the OCP curves for the uncoated and coated 316L stainless steel samples for both tested environments 0.6 mol $L^{-1}$ NaCl solution and artificial solution, respectively. All the tested samples displayed a stable behaviour during the first 2 h of immersion on both solutions (see **Figure 9 (a)** and **(b)**). Additionally, is possible to verify a shifting on the $E_{corr}$ for more negative values on the coated samples which, in a first time, indicating that the thin films lead the 316L stainless steel to a higher susceptibility to corrosion processes. As discussed by Moreto and colleagues **[62]**, in general the $E_{corr}$ indicates the material's nobility and more positive values imply on a more corrosion-resistance system. In addition, the authors mentioned that the $E_{corr}$ is an indicative and as so is not capable of fully describe the behaviour of an electrochemical system once several factors can affect the $E_{corr}$ values.

In this context, the utilisation of more comprehensive electrochemical techniques is essential. Considering the PPc for all specimens tested in 0.6 mol $L^{-1}$ NaCl solution, it can be verified that the $Nb_2O_5$ coating increased the $E_{corr}$ and reduced the corrosion current ($i_{corr}$) when compared to the base material (-0.05 *versus* -0.20 V/SCE and 0.0059 *versus* 0.012 µA $cm^{-2}$), see **Figure 10**. These findings demonstrated the significant enhancement achieved through the functionalisation of 316L stainless steel by reactive sputtering technique, as the $Nb_2O_5$ coating could reduce the $i_{corr}$ value by nearly 50% and the $E_{corr}$ by 75%. Regarding the 316L stainless steel/a-C coating, the $E_{corr}$ value, even though lower, is very similar to the 316L stainless steel (-0.26 V/SCE) and the $i_{corr}$ diminished (0.0089 µA $cm^{-2}$), indicating a positive result in terms of corrosion protection. Considering the artificial saliva solution, see **Figure 11**, the same positive effect of

implementing the thin films was observed, were for the $Nb_2O_5$ shifted the $E_{corr}$ to more positive values (-0.13 V/SCE) and reduced the $i_{corr}$ (0.0055 μA $cm^{-2}$) in comparison to the uncoated 316L stainless steel (-0.20 V/SCE and 0.0176 μA $cm^{-2}$). Additionally, the a-C coating promoted a lower, but relevant, protective effect in comparison to the $Nb_2O_5$ thin film, increasing the $E_{corr}$ (-0.14 V/SCE) and diminishing the $i_{corr}$ (0.011 μA $cm^{-2}$). After obtaining the PP tests, a series of optical images were performed to evaluate the topography of the corroded surfaces. An analysis of the material topography following the PPc tests further corroborates the positive impact of both coatings on the corrosion resistance of 316L stainless steel. As can be seen, the 316L stainless steel samples exhibited corroded areas across the metallic surface, whereas the coated samples showed only a few delaminations in the $Nb_2O_5$ coating and some small pits, even after the large damage to the coating, in the a-C film. It is important to note that, like the observations made during the wear tests, the a-C thin film exhibited multiple cracks and instances of delamination because of its exposure to aggressive environments. This phenomenon can be attributed to the relatively lower corrosion and wear resistance of the a-C coating when compared to $Nb_2O_5$, which successfully maintained its integrity even after undergoing extensive electrochemical and wear analyses.

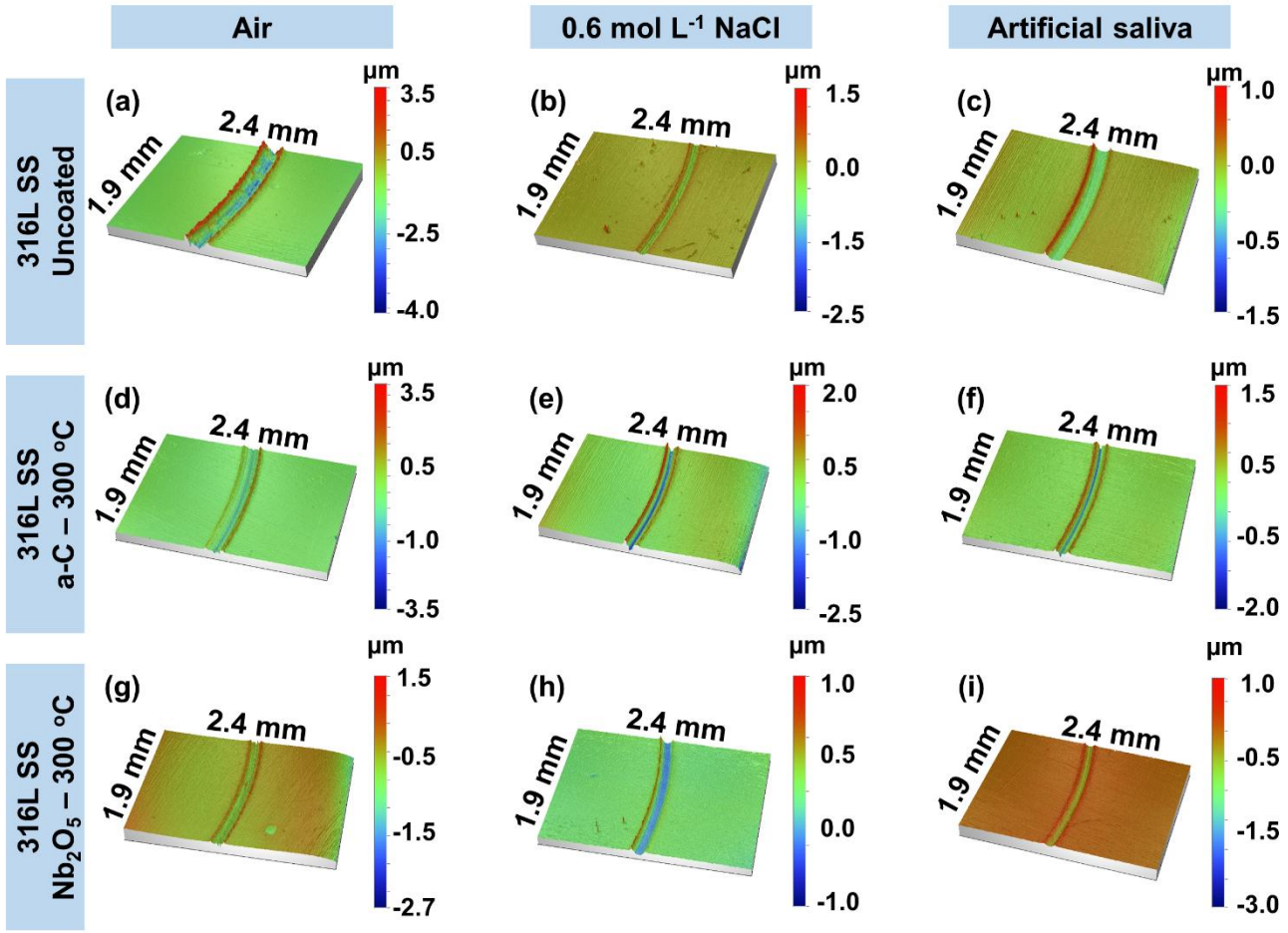


**Figure 8.** Wear track profilometry analysis for the 316L stainless steel, 316L stainless steel/a-C and 316L stainless steel/$Nb_2O_5$ samples after the first 300 s on the pin-on-disk analysis for **(a,d,g)** air, **(b,e,h)** after 2 h immersion in 0.6 mol $L^{-1}$ NaCl and **(c,f,i)** 2 h immersion in saliva artificial.

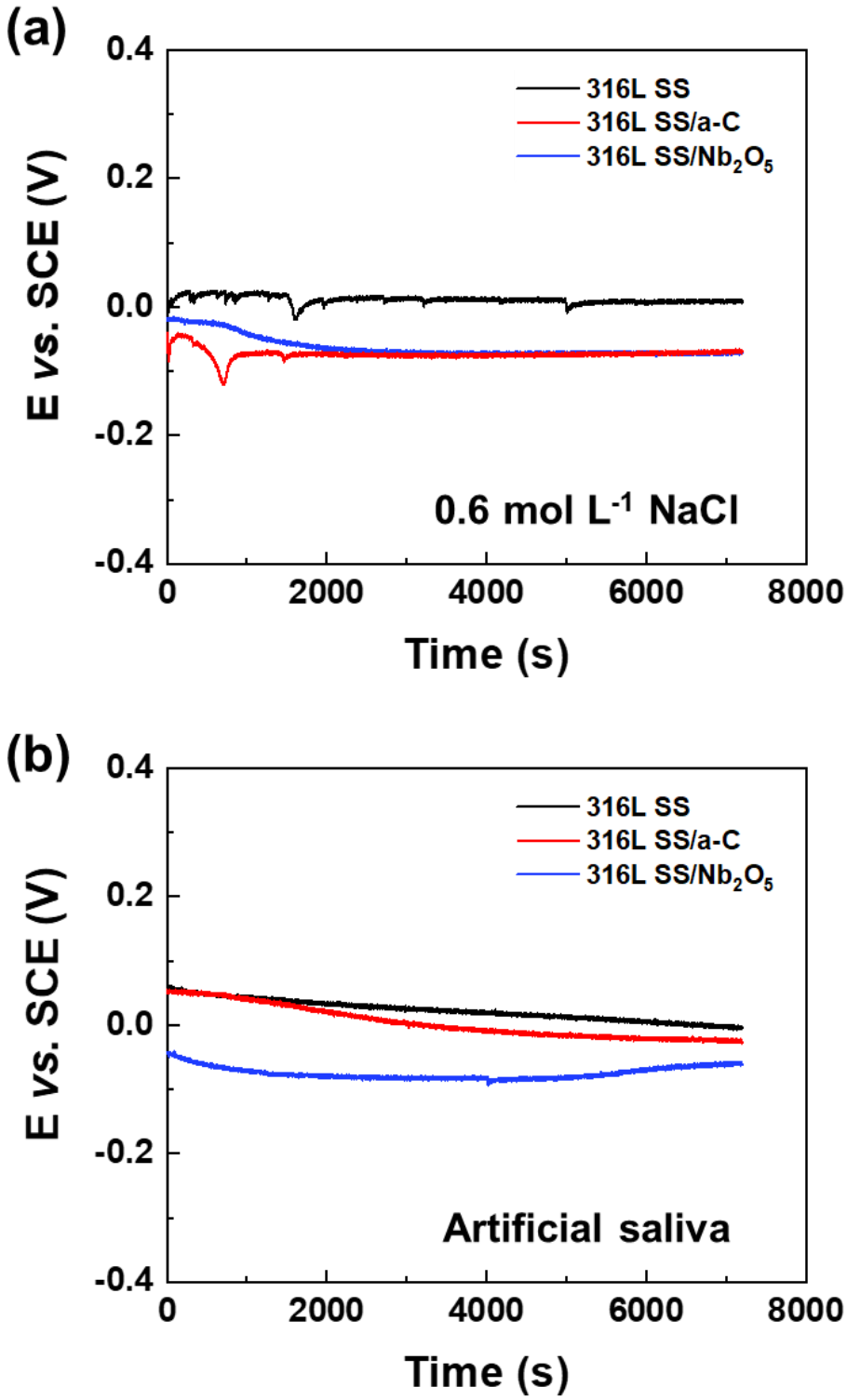


**Figure 9.** OCP curves for the 316L stainless steel, 316L stainless steel/a-C and 316L stainless steel/$Nb_2O_5$ samples for the first 2 h of immersion: **(a)** 0.6 mol $L^{-1}$ NaCl solution and **(b)** artificial saliva solution.

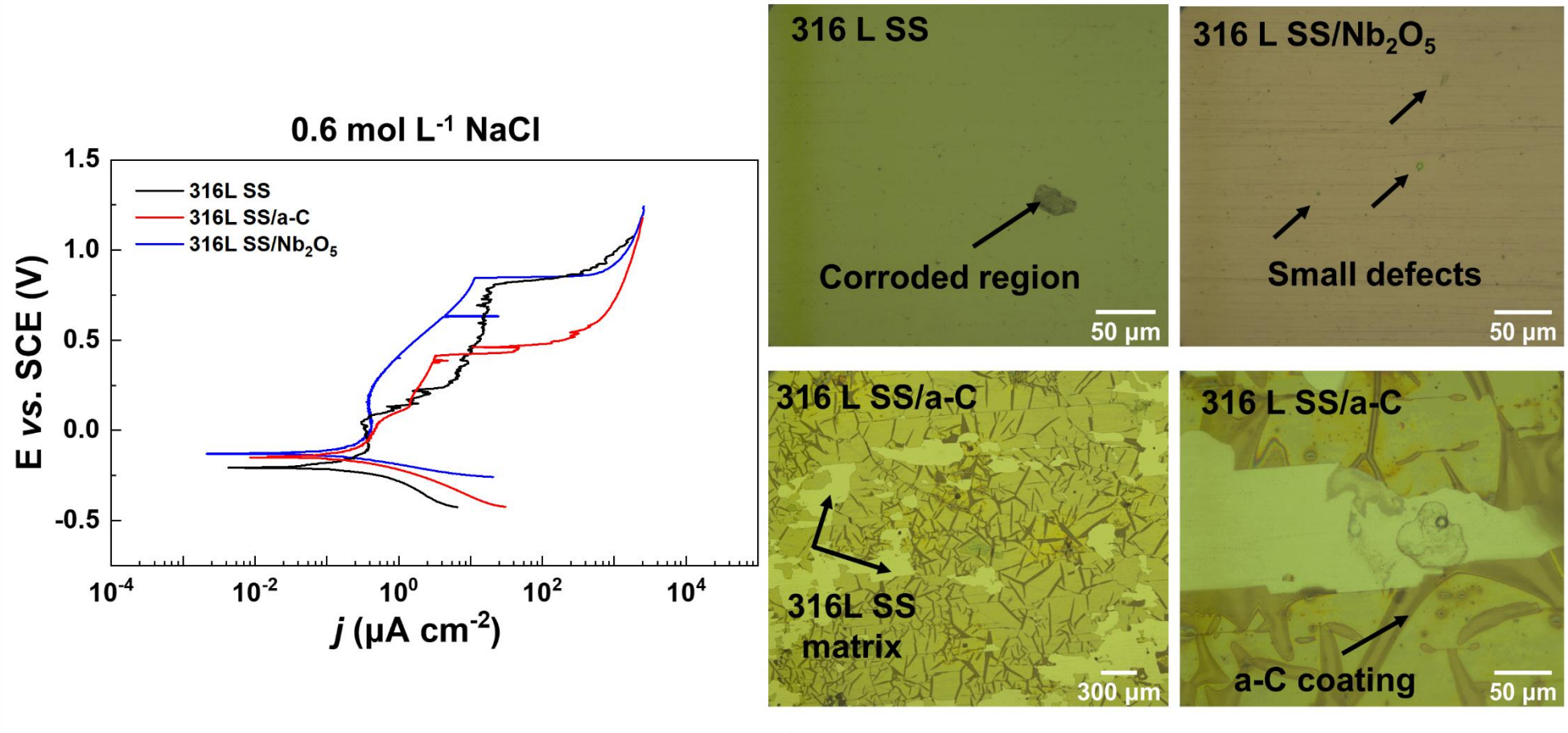


**Figure 10.** PPc curves and the corresponding optical images for the 316L stainless steel uncoated and coated with $Nb_2O_5$ and a-C films following the corrosion tests in a 0.6 mol $L^{-1}$ NaCl solution.

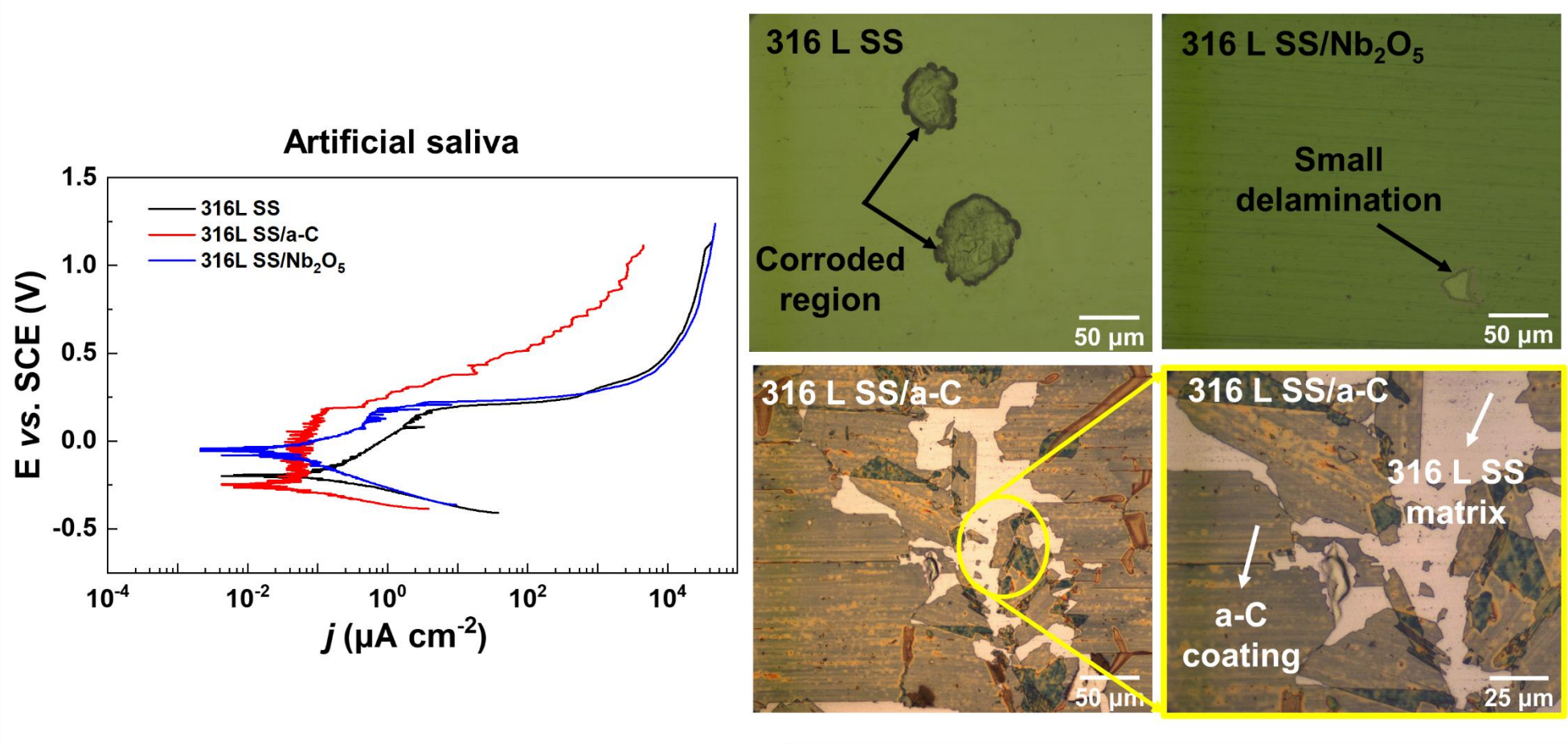


**Figure 11.** PPc curves and the corresponding optical images for the 316L stainless steel uncoated and coated with $Nb_2O_5$ and a-C films following the corrosion tests in artificial saliva solution.

**Figures 12 (a-d)** display a comparison of the Bode plots and Nyquist diagrams for the 316L stainless steel, 316L stainless steel/a-C, and 316L stainless steel/$Nb_2O_5$ samples after the first 2 h of immersion in both 0.6 mol $L^{-1}$ NaCl and artificial saliva solutions. It is clear from the Bode plots, see **Figure 12 (a)** and **12 (c)**, that the 316L stainless steel/$Nb_2O_5$ sample exhibited the highest overall corrosion resistance, indicated by the greatest impedance modulus, followed by the 316L stainless steel/a-C and 316L stainless steel samples, respectively. These findings align with the studies by Ferreira et al and Moreto et al **[49,62]**, which underscore the beneficial impact of sputtered thin films on corrosion resistance for different metallic materials. A comprehensive analysis of the EIS spectra reveals the presence of two distinct time constants: one observed at low frequencies, which is associated with localised corrosion processes occurring in both coated and uncoated 316L stainless steel substrates, and another at high frequencies, which is related to the behaviour of the oxide coatings. With respect to the Nyquist diagrams (see **Figure 12 (b)** and **12 (d)**), both coatings significantly enhanced the corrosion resistance of the 316L stainless steel, as evidenced by the increase in the semi-circular arc. Ultimately, the corrosion tests provided compelling evidence of the efficacy of reactive sputtering in creating coatings that markedly improve the corrosion resistance of 316L stainless steel. It is important to emphasise that all this evidence was also corroborated by the wear tests.

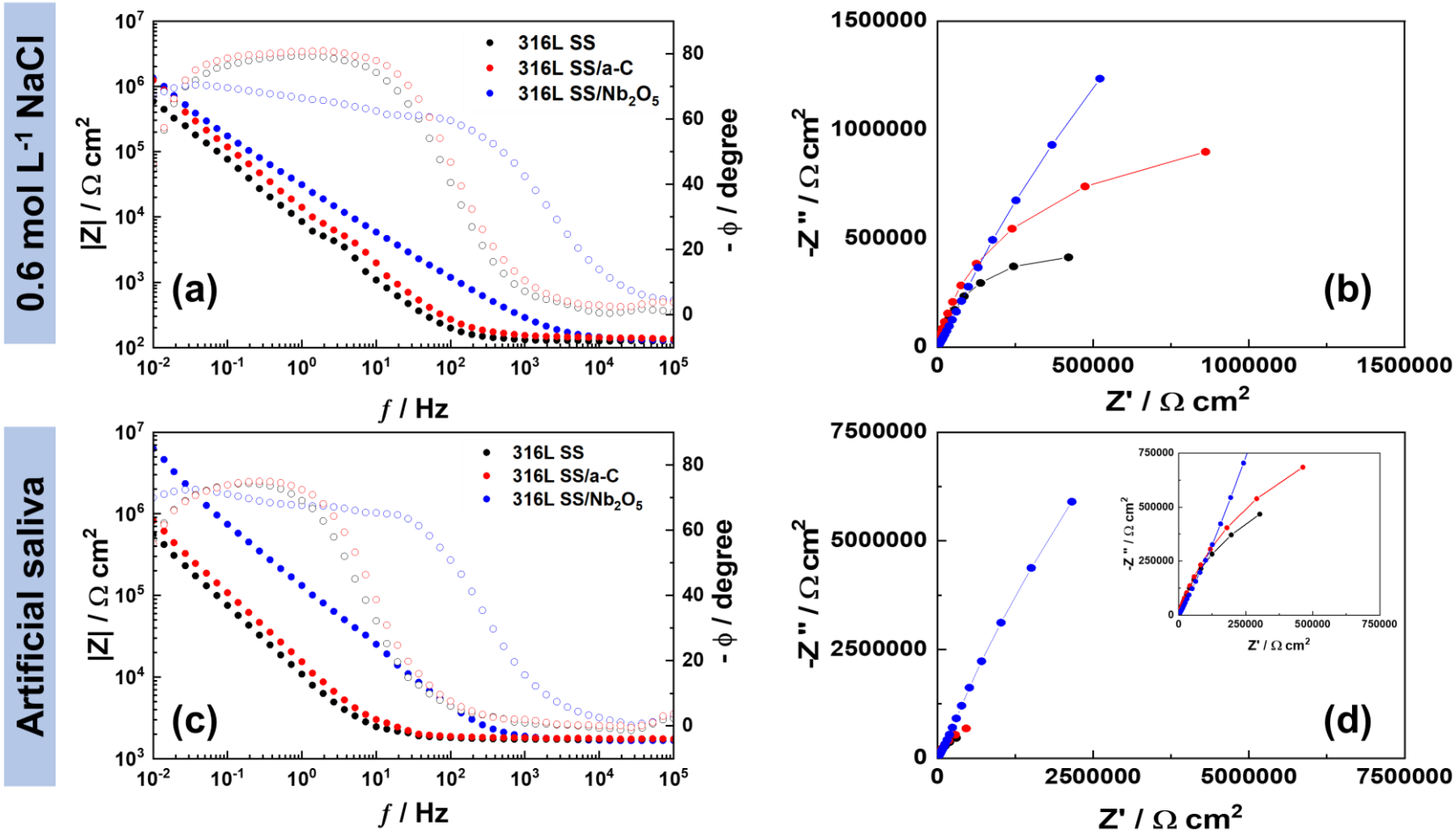


**Figure 12.** Nyquist diagrams and Bode plots for the 316L stainless steel, 316L stainless steel/a-C and 316L stainless steel/$Nb_2O_5$ samples for the first 2 h of immersion **(a,b)** 0.6 mol $L^{-1}$ NaCl and **(c, d)** artificial saliva solution.

## 4. Conclusions

This investigation examined the influence of surface functionalisation, employing $Nb_2O_5$ and a-C coatings, upon the wear and corrosion behaviour of 316L stainless steel. The main results are summarised as follows:

§ Reactive sputtering proved highly effective in producing nanostructured $Nb_2O_5$ and a-C coatings on the 316L stainless steel surfaces at 300 ºC, significantly enhancing wear and corrosion resistance.

§ The superior tribological performance of both coatings was evident across a range of test environments (air, 0.6 mol $L^{-1}$ NaCl solution, and artificial saliva solution), with significantly reduced coefficients of friction compared to the uncoated alloy, reaching up about 50% for both coatings.

§ The $Nb_2O_5$ and a-C coatings significantly reduced the wear rate compared to the uncoated material under all analysed conditions, achieving approximately 90% and 60%, respectively. Furthermore, even under severe wear conditions, the $Nb_2O_5$ thin film remained intact, demonstrating excellent adhesion and its ability to protect the 316L stainless steel substrate

§ Considering sodium chloride environment, corrosion protection was significantly enhanced by the $Nb_2O_5$ coating, as indicated by an increased $E_{corr}$ (-0.05 V/SCE *versus* -0.20 V/SCE) and reduced $i_{corr}$ (0.0059 µA $cm^{-2}$ *versus* 0.012 µA $cm^{-2}$) compared to the uncoated 316L stainless steel. The a-C coating also showed a reduction in $i_{corr}$ (0.0089 µA $cm^{-2}$), despite a similar $E_{corr}$ (~ -0.26 V/SCE);

§ Electrochemical analysis in artificial saliva revealed that the $Nb_2O_5$ coating displayed a substantially more positive corrosion potential ($E_{corr}$ = - 0.13 V/SCE *versus* -0.20 V/SCE) and a considerably lower corrosion current ($i_{corr}$ = 0.0055 µA $cm^{-2}$ *versus* 0.0176 µA $cm^{-2}$) when compared to the base alloy. The a-C coating demonstrated a lower level of corrosion protection than the 316L stainless steel/ $Nb_2O_5$ coating. Nevertheless, it exhibited superior resistance to uniform corrosion process when compared to the uncoated material, with a measured $E_{corr}$ of approximately -0.14 V/SCE and an $i_{corr}$ of 0.011 µA $cm^{-2}$;

§ These findings highlight the significant potential of $Nb_2O_5$ and a-C coatings to improve the wear and corrosion resistance of 316L stainless steel, thereby prompting further research into optimised surface treatments to enhance its durability in demanding applications in the biomedical sector.

**Conflict of interest**

The authors declare that they have no known competing financial interests or personal relationships that could have appeared to influence the work reported in this paper.

**Data availability**

Not applicable

**Code availability**

Not applicable

## 5. References


1. A. Ruggiero, M. de Stefano, Experimental investigation on the bio-tribocorrosive behavior of Ti-6Al-4V alloy and 316L stainless steel in two biological solutions. Tribol. Int. **190**, 109033 (2023). https://doi.org/10.1016/j.triboint.2023.109033.
2. M.E. Aksoy, B. Aksakal, N. Aslan, B. Dikici, Enhanced adhesion and corrosion properties of boron doped bioceramic coated 316L implants. Prot. Met. Phys. Chem. Surf. **57**, 1040–1050 (2021). https://doi.org/10.1134/S2070205121050026.
3. M.S. Jadon, G. Bhanjana, N. Dilbaghi, N.K. Singhal, S. Kumar, Fabrication and evaluation of silver-doped magnesium oxide nanocomposite coatings for orthopaedics applications. J. Alloys Compd. **972**, 172848 (2024). https://doi.org/10.1016/j.jallcom.2023.172848.
4. A. Hatem, J. Lin, R. Wei, R.D. Torres, C. Laurindo, P. Soares, Tribocorrosion behavior of DLC-coated Ti-6Al-4V alloy deposited by PIID and PEMS + PIID techniques for biomedical applications. Surf. Coat. Technol. **332**, 223–232 (2017). https://doi.org/10.1016/j.surfcoat.2017.07.004.

5. I. Pana, A. Vladescu, L.R. Constantin, I.G. Sandu, M. Dinu, C.M. Cotrut, In Vitro Corrosion and Tribocorrosion Performance of Biocompatible Carbide Coatings. Coatings. **10**, 654 (2020). https://doi.org/10.3390/coatings10070654.
6. S.M. Muthu, C. Mohana Bharathi, N. Vishal Gukhan, S. Vignesh Kumar, M. Venkatesh Kannan, M. Arivarasu, M. Manikandan, N. Arivazhagan, Hot Corrosion Studies on Dissimilar Weldments C-22 and AISI 316L in the Molten Salt $K_2SO_4$ + 60%wt NaCl Environment. Mater. Today Proc. **5**, 13340–13346 (2018). https://doi.org/10.1016/j.matpr.2018.02.326.
7. Q. Chen, G.A. Thouas, Metallic implant biomaterials. Mater. Sci. Eng. R Rep. **87**, 1–57 (2015). https://doi.org/10.1016/j.mser.2014.10.001.
8. B. Mi, H. Wang, Q. Wang, J. Cai, Z. Qin, Z. Chen, Corrosion resistance and contact resistance properties of Cr-doped amorphous carbon films deposited under different carbon target current on the 316L stainless steel bipolar plate for PEMFC. Vacuum. **203**, 111263 (2022). https://doi.org/10.1016/j.vacuum.2022.111263.
9. J. Liu, T. Zhang, G. Meng, Y. Shao, F. Wang, Effect of pitting nucleation on critical pitting temperature of 316L stainless steel by nitric acid passivation. Corros. Sci. **91**, 232–244 (2015). https://doi.org/10.1016/j.corsci.2014.11.018.
10. D. Lindell, R. Pettersson, Crystallographic effects in corrosion of austenitic stainless steel 316L. Mater. Corros. **66**, 727–732 (2015). https://doi.org/10.1002/maco.201408002.
11. N.S. Al-Mamun, W. Haider, I. Shabib, Corrosion resistance of additively manufactured 316L stainless steel in chloride−thiosulfate environment. Electrochim. Acta. **362**, 137039 (2020). https://doi.org/10.1016/j.electacta.2020.137039.
12. M.J.K. Lodhi, K.M. Deen, M.C. Greenlee-Wacker, W. Haider, Additively manufactured 316L stainless steel with improved corrosion resistance and biological response for biomedical applications. Addit. Manuf. **27**, 8–19 (2019). https://doi.org/10.1016/j.addma.2019.02.005.
13. Xiejunjun, Wangao, Yuanyongliang, Gaoyang, Corrosion Behavior of 316L Stainless Steel Weld under Constant Strain. J. Phys. Conf. Ser. **1653,** 012035 (2020). https://doi.org/10.1088/1742-6596/1653/1/012035.
14. L. Reclaru, Corrosion behavior of a welded stainless-steel orthopedic implant. Biomaterials. **22**, 269–279 (2001). https://doi.org/10.1016/S0142-9612(00)00185-X.
15. B.B. Ramos, F.A. Vicente, G. Hammes, T. Bendo, C. Binder, Enhancing corrosion and tribology performance of stainless steel with DLC coatings: Effects of doping and

multilayered structures. Surf. Coat. Technol. **477**, 130334 (2024). https://doi.org/10.1016/j.surfcoat.2023.130334.

16. A.M. Ralls, P.L. Menezes, Revealing the fretting corrosion mechanisms of laser shock peened cold spray 316L stainless steel. Tribol. Int. **192**, 109227 (2024). https://doi.org/10.1016/j.triboint.2023.109227.
17. I. Atmaca, B. Dikici, K.V. Ezirmik, A. G. Bulutsuz, M. Niinomi, Investigation of corrosion and wear performance of TiNbTaZr/Cr-Mo PVD coatings on 316L SS in Hanks's solution for improved biomedical applications. Surf. Coat. Technol. **473**, 130021 (2023). https://doi.org/10.1016/j.surfcoat.2023.130021.
18. Y. Jian, C. Yang, J. Zhang, L. Qi, X. Shi, H. Deng, Y. Du, One-step electrodeposition of Janus chitosan coating for metallic implants with anti-corrosion properties. Colloids Surf. A Physicochem. Eng. Aspects. **641**, 128498 (2022). https://doi.org/10.1016/j.colsurfa.2022.128498.
19. F. H. Laybidi, A. Bahrami, Antibacterial properties of ZnO-containing bioactive glass coatings for biomedical applications. Mat. Lett. **365**, 136433 (2024). https://doi.org/10.1016/j.matlet.2024.136433.
20. N. Bouydia, H. Atmani, M. Boulghallat, A. Jouaiti, L. Laallam, Electrochemical Study and Characterization: Exploration and Analysis of Electrodeposition of Hydroxyapatite on 316L Stainless Steel in A Physiological Environment. Anal. Bioanal. Electrochem. **16**, 1 (2024). https://doi.org/10.22034/abec.2024.711556.
21. A. Imran, R.A. Malik, H. Alrobei, M.A. U. Rehman, Electrophoretic deposition of polyetheretherketone/polytetrafluoroethylene on 316L SS with improved tribological and corrosion properties for biomedical applications. Front. Mater. **11**, 1473032 (2024). https://doi.org/10.3389/fmats.2024.1473032.
22. I. Herath, J. Davies, G. Will, P.A. Tran, A. Velic, M. Sarvghad, M. Islam, P.K. Paritala, A. Jaggessar, M. Schuetz, K. Chatterjee, P.K.D.V. Yarlagadda, Anodization of medical grade stainless steel for improved corrosion resistance and nanostructure formation targeting biomedical applications. Electrochim. Acta. **416**, 140274 (2022). https://doi.org/10.1016/j.electacta.2022.140274.
23. B. Zhang, H. Ni, R. Chen, W. Zhan, C. Zhang, R. Lei, Y. Zha, A two-step anodic method to fabricate self-organised nanopore arrays on stainless steel. Appl. Surf. Sci. **351**, 1161–1168 (2015). https://doi.org/10.1016/j.apsusc.2015.06.083.
24. A.K. Nunach, G. Rani, R. Ahlawat, H. Kumar, Evaluation of Boerhaavia diffusa roots extract as a sustainable corrosion inhibitor for mild steel in sulfuric acid

environments. Vietnam J. Chem. **1**, (2024) 202400159. https://doi.org/10.1002/vjch.202400159.

25. A.K. Nunach, G. Rani, R. Ahlawat, Corrosion Inhibition Potential of Cymbopogon citratus (Lemongrass) Leaves Extract on Mild Steel in 0.1 M Sulphuric Acid Medium at Different Temperatures. Ajc. **35**, 1810–1818 (2023). https://doi.org/10.14233/ajchem.2023.27966.
26. L.R. Kanyane, T.J. Malepe, N. Malatji, A.P.I. Popoola, Synthesis and Characterization of Al–SiC Composite Coatings on 316L Stainless Steel Fabricated via Laser Cladding Technique. Metallogr. Microstruct. Anal. **10**, 601–609 (2021). https://doi.org/10.1007/s13632-021-00778-y.
27. K. Harenharen, S. P. Kumar, T. Panneerselvam, P. D. Babu, N. Srinaman, Investigating the effect of laser shock peening on the wear behaviour of selective laser melted 316L stainless steel. Opt. Laser Technol. **162**, 109317 (2023). https://doi.org/10.1016/j.optlastec.2023.109317.
28. Z. Su, X. Jie, W. Li, Z. Liao, Y. Li, W. Zhu, Effect of $C_2H_2$ flow rate and a Ti/TiN/TiCN interlayer on the structure, mechanical and tribological properties of a-C:H films deposited using a hybrid PVD/PECVD process with an anode-layer ion source. Vacuum. **209**, 111753 (2023). https://doi.org/10.1016/j.vacuum.2022.111753.
29. L.S. Vaca, J.P. Quintana, D. Vega, A. Márquez, S.P. Brühl, Tribological and corrosion behavior of duplex coated AISI 316L using plasma-based ion implantation and deposition. Mater. Today Commun. **26**, 101892 (2021). https://doi.org/10.1016/j.mtcomm.2020.101892.
30. J.A. Moreto, R.V. Gelamo, M.V. Da Silva, T.T. Steffen, C.J.F. Oliveira, P.A. A. Buranello, M.R. Pinto, New insights of $Nb_2O_5$-based coatings on the 316L SS surfaces: enhanced biological responses. J. Mater. Sci. Mater. Med. **32**, 25 (2021). https://doi.org/10.1007/s10856-021-06498-7.
31. M.O.A. Ferreira, V.A.F. Morgado, K.R. dos Santos, R.V. Gelamo, F.E. Mariani, N.B.L. Slade, M.M. Morais, C.A. Fortulan, R. Galo, R.G. Jasinevicius, H.C. Pinto, J.A. Moreto, Enhancing the Wear Performance of 316L Stainless Steel with $Nb_2O_5$ Coatings Deposited via DC Sputtering at Room Temperature under Varied Environmental Conditions. Lubricants. **12**, 345 (2024). https://doi.org/10.3390/lubricants12100345.
32. M. Ammam, Electrophoretic deposition under modulated electric fields: a review. RSC Adv. **2**, 7633 (2012). https://doi.org/10.1039/c2ra01342h.

33. A. Jaafar, C. Hecker, P. Árki, Y. Joseph, Sol-Gel Derived Hydroxyapatite Coatings for Titanium Implants: A Review. Bioengineering. **7**, 127 (2020). https://doi.org/10.3390/bioengineering7040127.
34. M. Tharmaraj, A. Radhakrishnan, A. Ramani, N. Srinivasan, Investigation and In Vitro Studies of a $ZrO_2$/g-$C_3$ $N_4$ Composite Coated on 316L Stainless Steel for Biomedical Applications. Mat. Corros. **1**, 202414525 (2024). https://doi.org/10.1002/maco.202414525.
35. H. Sirajunisha, T. Balakrishnan, P. Sakthivel, A. Krishnaveni, Enhanced corrosion resistance, antibacterial and biological properties of sol-gel derived Ti-rGO-HAp nanocomposites. Chem. Phys. Impact. **6,** 100159 (2023). https://doi.org/10.1016/j.chphi.2022.100159.
36. M.T. Mohammed, A.H. Lafta, F.Q. Mohammed, Surface Characterization of Pure and Composite Sol-gel Nano-coatings Deposited on 316L Stainless Steel for Hard Tissue Replacements. Mat. Res. **26**, e20220479 (2023). https://doi.org/10.1590/1980-5373-mr-2022-0479.
37. R.M. Almeida, M.C. Gonçalves, Sol–Gel Process and Products. Wiley. **1**, (2021) 969–979. https://doi.org/10.1002/9781118801017.ch8.2.
38. L. Wang, C. Wang, S. Wu, Y. Fan, X. Li, Influence of the mechanical properties of biomaterials on degradability, cell behaviors and signaling pathways: current progress and challenges. Biomater. Sci. **8**, 2714–2733 (2020). https://doi.org/10.1039/D0BM00269K.
39. M.M. Nair, S. Swaroop, Impact of the oxide layer and subsurface micromechanical properties of laser peened 31L stainless steel on biocorrosion resistance in simulated body fluid. Surf. Interfaces. **56**, 105672 (2025). https://doi.org/10.1016/j.surfin.2024.105672.
40. M.R.P. Kumar, S.T. Siddeswar, S. Elanchezian, K. Yogesh, T. Dharun, Experimental investigation on the superhydrophobic property of laser micromachined stainless steel 316L surface. Mater. Today Proc. **98**, 153–159 (2024). https://doi.org/10.1016/j.matpr.2023.10.038.
41. V.D.S. Neves, F.Q. Correa, M.O.A. Ferreira, A.R. Rodrigues, W. Wolf, R. Galo, F.M.M. Yasuoka, J.A. Moreto, The Use of Nanosecond Pulsed Fibre Laser Treatment to Improve the Corrosion Resistance of 316L SS Utilised as Surgical Devices. Materials. **17**, 6178 (2024). https://doi.org/10.3390/ma17246178.

42. M.C. A. Bino, W.A. Eurídice, R.V. Gelamo, N.B. Leite, M.V. Silva, A. Siervo, M.R. Pinto, P.A.A. Buranello, J.A. Moreto, Structural and morphological characterization of $Ti_6Al_4V$ alloy surface functionalization based on $Nb_2O_5$ thin film for biomedical applications. Appl. Surf. Sci. **557**, 149739 (2021). https://doi.org/10.1016/j.apsusc.2021.149739.
43. J.P.L. Nascimento, M.O.A. Ferreira, R.V. Gelamo, J. Scarmínio, T.T. Steffen, B.P. Da Silva, I.V. Aoki, A.G. Santos, V.V. Castro, C. F. Malfatti, J.A. Moreto, Enhancing the corrosion protection of Ti-6Al-4V alloy through reactive sputtering niobium oxide thin films. Surf. Coat. Tech. **428**, 127854 (2021). https://doi.org/10.1016/j.surfcoat.2021.127854.
44. J.P.L. Nascimento, L. R. Freitas, C.N. Lemos, R.V. Gelamo, J.A. Moreto, A New View of a:C-H-coated Ti-6Al-4V Alloy to be Used as Orthopedic Implants: Influence of Surface Free-energy of Interaction on the Biological Responses. Orbital Electron. J. Chem. **13**, 264–268 (2021). http://dx.doi.org/10.17807/orbital.v13i3.1622.
45. T.I. Silva, M.O.A. Ferreira, J.P.L. Nascimento, L.R. Pietro, L.A.R.C. Neto, H.C. Moreira, L.V. Pereira, N.B. Leite, R.V. Gelamo, J.A. Moreto, Development of a Low-Cost Ball-on-Flat Linear Reciprocating Apparatus: Test Validation Using Ti-6Al-4V and Ti-6Al-4V/$Nb_2O_5$ Coatings. J. Mater. Sci. Technol. Res. **9**, 43–52 (2022). https://doi.org/10.31875/2410-4701.2022.09.05.
46. W.A. Eurídice, N.B. Leite, R.V. Gelamo, P.A.A. Buranello, M.V. Silva, C.J.F. Oliveira, R.F.V. Lopez, C.N. Lemos, A. Siervo, J.A. Moreto, a-C:H films produced by PECVD technique onto substrate of Ti6Al4V alloy: Chemical and biological responses. Appl. Surf. Sci. **503**, 144084 (2020). https://doi.org/10.1016/j.apsusc.2019.144084.
47. M.O.A. Ferreira, K.R. dos Santos, D.G. Bon, R.V. Gelamo, R. Galo, N.B. Leite, C.A.R.P. Baptista, H.C. Pinto, J.A. Moreto, The positive impact of the reactive sputtered nanostructured $Nb_2O_5$ coatings to reduce the FCG rates of the 2524-T3 alloy in an aggressive medium, Emergent Mater. **7**, 2129–2141 (2024). https://doi.org/10.1007/s42247-024-00746-6.
48. R.V. Gelamo, N.B. Leite, N. Amadeu, M.R.P.M. Tavares, D. Oberschmidt, S. Klemm, C. Fleck, C.T. Cakir, M. Radtke, J.A. Moreto, Exploring the $Nb_2O_5$ coating deposited on the Ti-6Al-4V alloy by a novel GE-XANES technique and nanoindentation load-depth, Mater. Lett. **355**, 135584 (2024). https://doi.org/10.1016/j.matlet.2023.135584.

49. M.O.A. Ferreira, F.E. Mariani, N.B. Leite, R.V. Gelamo, I.V. Aoki, A. Siervo, H.C. Pinto, J.A. Moreto, Niobium and carbon nanostructured coatings for corrosion protection of the 316L stainless steel. Mater. Chem. Phys. **312**, 128610 (2024). https://doi.org/10.1016/j.matchemphys.2023.128610.
50. A. Fróis, J.R. Marques, L. Santos, M. Peres, K. Lorenz, C.S. Louro, A.C. Santos, Metal Release and Cell Viability of 316L Stainless Steel Sputter-Coated with N-Doped a-C:H Coatings. Appl. Sci. **14**, 10500 (2024). https://doi.org/10.3390/app142210500.
51. E. Dobruchowska, J. Schulz, V. Zavaleyev, J. Walkowicz, T. Suszko, B. Warcholinski, Influence of the Metallic Sublayer on Corrosion Resistance in Hanks' Solution of 316L Stainless Steel Coated with Diamond-like Carbon. Materials. **17**, 4487 (2024). https://doi.org/10.3390/ma17184487.
52. S.P. Murugan, G. George, J. Jaisingh, Wear performance of Ti-based alloy coatings on 316L SS fabricated with the sputtering method: Relevance to biomedical implants. BME. **35**, 219–235 (2024). https://doi.org/10.3233/BME-230127.
53. T.C. Senocak, K.V. Ezirmik, F. Aysin, N. Simsek Ozek, S. Cengiz, Niobium-oxynitride coatings for biomedical applications: Its antibacterial effects and in-vitro cytotoxicity. Mater. Sci. Eng. C. **120**, 111662 (2021). https://doi.org/10.1016/j.msec.2020.111662.
54. American Society for Testing and Materials. ASTM E99-23. **99**, 2959 (2023) http://dx.doi.org/10.1520/G0099-17.
55. K. Ahmad, S.A. Batool, M.T. Farooq, B. Minhas, J. Manzur, M. Yasir, A. Wadood, E. Avcu, M.A.U. Rehman, Corrosion, surface, and tribological behavior of electrophoretically deposited polyether ether ketone coatings on 316L stainless steel for orthopedic applications. J. Mech. Behav. Biomed. Mater. **148**, 106188 (2023). https://doi.org/10.1016/j.jmbbm.2023.106188.
56. U.T. Vinothraj, M. A. Xavior, Wear and Frictional Behaviour of Additive Manufactured SS 316L Through Powder Bed Fusion, Appl. Sci. Eng. **27**, 1 (2024). https://doi.org/10.6180/jase.202412_27(12).0001.
57. H. Chen, R.P. Li, S. Guo, Z. Zhang, X.X. Li, X.L. Zhao, Microstructure and tribocorrosion behaviors of Fe–Al–Ti coatings prepared by the aluminothermic reaction. Wear. **530**, 205055 (2023). https://doi.org/10.1016/j.wear.2023.205055.

58. S. Cao, Z. Xu, X. Zhang, Y. Fan, Tribocorrosion behavior of 316L stainless steel sliding against different ceramics in 0.5 M $H_2SO_4$ solution. Tribol. Int. **190**, 109032 (2023). https://doi.org/10.1016/j.triboint.2023.109032.
59. E. Ghio, G. Bolelli, A. Bertè, E. Cerri, Diamond-Like Carbon (DLC) and AlCrN films onto Ti-6Al-4V substrates by Laser-Powder Bed Fusion (L-PBF): Effect of substrate heat treatment and surface finish. Surf. Coat. Tech. **475**, 130128 (2023). https://doi.org/10.1016/j.surfcoat.2023.130128.
60. M.J. Lima, T. Vuchkov, F. Ferreira, D. Cavaleiro, A. Costa, A. Cavaleiro, S. Carvalho, PVD coatings on punches for low interfacial adhesion to pharmaceuticals. Surf. Coat. Tech. **472**, 129860 (2023). https://doi.org/10.1016/j.surfcoat.2023.129860.
61. R. Song, S. Chen, Z. Liu, C. Huo, Q. Chen, Effect of W-doping on the structure and properties of DLC films prepared by combining physical and chemical vapor deposition. Diam. Relat. Mater. **132**, 109687 (2023). https://doi.org/10.1016/j.diamond.2023.109687.
62. J.A. Moreto, C.E.B. Marino, W.W.B. Filho, L.A. Rocha, J.C.S. Fernandes, SVET, SKP and EIS study of the corrosion behaviour of high strength Al and Al–Li alloys used in aircraft fabrication. Corros. Sci. **84**, 30–41 (2014). https://doi.org/10.1016/j.corsci.2014.03.001.